UNIVERSITY OF THESSALY
DEPARTMENT OF MECHANICAL ENGINNERING

INVESTIGATION OF SOLIDIFICATION AND HOMOGENIZATION OF THE ALUMINUM ALLOY 6060

By

Anastasia Kotsiaridi

Supervisor Prof. Gregory N. Haidemenopoulos

Submitted to the Department of Mechanical Engineering on June 2021 in partial fulfillment of requirements for the degree of Mechanical Engineer

Thesis Committee:

1st member:	Prof. G.N. Haidemenopoulos
(Supervisor)	Department of Mechanical Engineering, University of Thessaly
2nd member:	Dr. A. Zervaki
	Department of Mechanical Engineering, University of Thessaly
3rd member:	Prof. A. Kermanidis
	Department of Mechanical Engineering, University of Thessaly

ABSTRACT

The evolution of phase fractions of intermetallic phases formed during solidification and homogenization of the Al-alloy 6060 observed computationally and experimentally. The aim of this project also, was the improvement of extrudability. After solidification, the as-cast billets contain several inhomogeneities, such as elemental and grain boundary segregation and formation of eutectic and intermetallic phases, which affect extrudability. So, homogenization process is required in order to increase the extrudability by the β-to-α AlFeSi transformation and elimination of the as-cast morphology. Additionally, the dissolution and re-precipitation of Mg_2Si during homogenization cooling is one of the main strengthening factors of the alloy.

The investigation includes simulations of solidification and cooling to room temperature, as well as homogenization heating, holding and cooling. The study also includes experimental observation of the as-cast and as-homogenized materials, via Optical Microscopy, SEM and EDX point analysis.

The simulation model and metallographies of the as-cast material present very good agreement and show that after solidification, α-AlFeSi, β-AlFeSi, Mg_2Si, π-phase and eutectic mixtures exist, which limit extrudability of the alloy. Also, elemental segregation near grain boundaries was identified.

The homogenization was simulated using two models (for homogenization temperatures, 570^{o}C and 580^{o}C respectively) because a difference between model predictions and experiments was observed regarding the completion of the β-to-α AlFeSi transformation. The difference can be attributed to temperature variation of the provided measurements obtained by industry. The updated simulation model for homogenization holding temperature 580^{o}C and experimental observations present very good agreement and show that the main phases after homogenization are Mg_2Si and α-AlFeSi, which improve extrudability. Also, elimination of elemental segregation observed. At the end, the increase of heating rate leads to complete transformation β-to-α AlFeSi and spheroidization of particles and the total homogenization time should be reduced.

TABLE OF CONTENTS

LIST OF FIGURES

LIST OF TABLES

ACKNOWLEDGEMENTS

For the completion of this Thesis, I would like to thank my thesis Supervisor, Prof. G.N. Haidemenopoulos, for his suggestions, guidance and advices during this project.

I would like to express my appreciation to John Aristeidakis and Maria-Ioanna Tzini for their infinite help and precious advices.

I would also like to thank Dr. Eleni Kamoutsi providing me the Optical Microscopy metallographies and SINTEF providing me the SEM and EDX point analysis of the as-cast and as-homogenized material.

I am grateful to Prof. A. Zervaki and Prof. A. Kermanidis for their guidance during the past years and for the serving in my thesis committee.
Last but not least, I wish to express my gratitude to my family and my friends for their support and my appreciation to Alexandros for his patience and encouragement.

1. INTRODUCTION

Aluminum extrusions are used in a variety of structural applications ranging from building and automotive to aerospace industries. The growing demand for weight-optimized design in order to reduce energy consumption and air pollution is a challenge for the automotive industry. Car companies try to respond with the design of new concept cars that include a light-weight design meet the requirements of the public with growing awareness on fuel consumption. The usage of Aluminum and Aluminum alloys is a promising field of study, that companies are investing more and more in. Low-density Al-alloys, especially age-hardenable Al-Mg-Si (6xxx) alloys, are a preferred choice, because of their combination of high strength, formability, extreme durability, excellent corrosion resistance and density.

6xxx Series alloys are heat-treatable, which means that they acquire their optimum mechanical properties through a process of thermal treatment. These are the Al-Mg-Si alloys (Mg and Si additions of around 1%) and are found widely throughout the welding fabrication, industry, used predominantly in the form of extrusions and incorporated in many structural components. The addition of magnesium and silicon to aluminum enables the formation of a magnesium-silicide intermetallic compound, which can contribute to precipitation strengthening through a solution heat treatment.

As shown in the triangle of the relation between the treatment, the properties and the microstructure, as depicted in *Figure 1*, the mechanical properties of an alloy are influenced by the microstructure, which depends on the thermomechanical treatments that a material has undergone. Thus, in order to achieve specific mechanical properties, it is necessary to control microstructural evolution via processing.

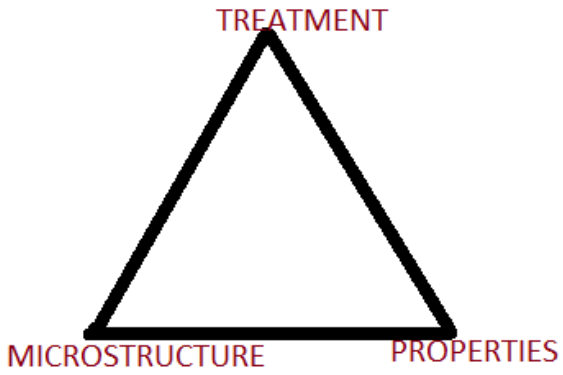

Figure 1: Triangle: Treatment-Microstructure-Properties.

In *Figure 2*, a sketch of the different process steps is depicted. First of all, the alloying elements of the alloy are added during *melt treatment*. The main strengthening is result of addition of Mg and Si to the formation of the intermetallic phase, Mg_2Si. Melt treatment is followed by casting. *Casting* is a technical process in which a molten metal acquires the desired shape (billet for rolling process or ingots for extrusion). The metal solidifies after the casting process. The microstructure of the

casting consists of three zones related to the size and morphology of the grains: chill, columnar and equiaxed zone.

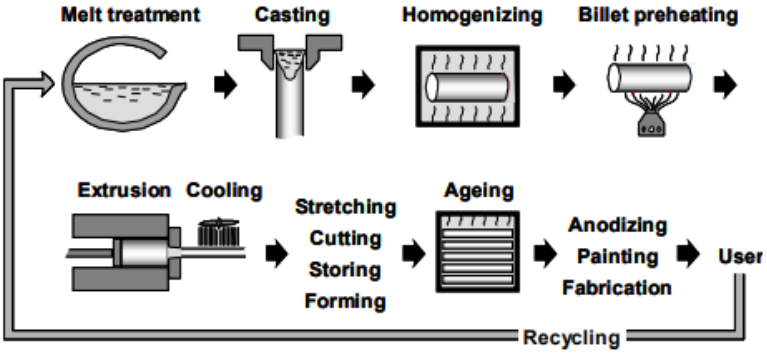

Figure 2: Sketch of the different process steps.

The solidification of the cast results to modification of the composition from point to point, i.e. segregation. Micro-segregation is found in composition changes in the dendritic regions due to the rejection of the second component and is more important at the borders of the columnar zone. Microsegregation is a significant problem in castings, because it affects the mechanical properties, due to the heterogeneity in the distribution of the alloying elements in the grain scale. This problem is more important when thermal treatments follow the casting to strengthen the alloy. In particular, in the alloys 6xxx the grains' inside lacks Mg, Si for the formation Mg_2Si during the process of precipitation. Also, β-AlFeSi, an intermetallic compound of Fe is a sharp microstructure that can cause cracking ruptures during extrusion. So, it needs to be transformed to a more desirable compound to increase extrudability of the material.

The next process is *homogenization*. During homogenization, the alloy is heated in order to uniformly dissolve the alloying elements in matrix. In this way the microstructure of Aluminum is transformed and especially alloying elements diffuse as intermetallics, formed near the grain boundaries during solidification and dissolve upon homogenization. Homogenization is followed by *quenching*, resulting in a supersaturated solid solution.

The 6xxx Aluminum alloys can be extruded. Prior to extrusion, the billet is *preheated* (450-500^{o}C) in order to reduce yield strength, dissolve Mg_2Si particles and permit extrusion to take place. *Extrusion* is a process used to create objects of fixed cross-sectional profile. The microstructure of Aluminum extrusion influences mechanical properties of the alloy and its surface quality. Wherever it is observed more plastic deformation, recrystallization can take place. Non-recrystallized structure is preferred, because large crystallized grains reduce formability and enhance Precipitation Free Zones (PFZ) during aging. Extrusion is followed by *quenching*, to avoid precipitation and maintain a supersaturated solid solution.

The final stage of heat treatments is aging. *Aging* is the process by which a uniform dispersion of precipitates is created from the supersaturated solid solution. Aging

determines final mechanical properties of the extruded profile. Based on all these treatments certain factors are controlled to obtain an alloy with a specific microstructure and the desired mechanical properties. Aging is a process that consists of many different steps-thermal cycles. The chain of treatments is solution annealing › quenching › storage › ageing (age hardening). Each step targets a different part of the age hardening mechanism that results to the final product. The general precipitation sequence in Al-Mg-Si alloys is:

SSSS → atomic clusters → GP zones → β´´ → β´, U1, U2, B´ →β, Si

Solution annealing targets the acquisition of the homogeneous solid state while after quenching, is expected the material to be into super saturate solid state (SSSS). During storage, the formation of atomic clusters and GP zones is expected, but storage temperature is crucial since very big clusters are unwanted. Age hardening is involved in the final three steps of the transformation and peak hardness achieved when transitioning from β´´to β´phase.

Homogenization is of the most important heat treatment applied in the production process of alloys 6xxx. Homogenization and the associated phase transformations have attracted increased attention due to the importance of the homogenization process in obtaining high extrudability and desirable properties in the extruded profiles. This project describes solidification and homogenization treatment and presents results from the simulation of the solidification and the homogenization of the Al-alloy 6060. Computational thermodynamic and kinetic modeling is used for the description of microstructural evolution during solidification and homogenization, aiming at the improvement of the final properties of 6060 Al-alloy.

The solidification and the homogenization processes have been studied by several researchers. Specific topics of interest are the microsegregation, the dissolution of Mg_2Si, the β-AlFeSi to α-AlFeSi transformation and the re-precipitation of Mg_2Si during homogenization cooling. The most important literature data concerning experimental and modeling studies are presented below.

Jim Hu et al studied the solidification of alloys with balanced and not balanced Mg and Si additions and with different alloying levels ranging from 6063 to 6082 and they researched the effects of growth rate, temperature gradient and composition on structure formation [1]. They observed that grain refinement is necessary to avoid columnar growth in alloys and that the transformations during cooling are important for the final structure and the materials properties. The microstructure evolution of the 6063 alloy during homogenization has been studied for various thermal cycles [2]. Microstructural changes during homogenization have been discussed for a 6063 alloy in [3], including the β-AlFeSi to α-AlFeSi transformation. It appears that the precipitation of the metastable β´-Mg_2Si phase instead of the equilibrium β-Mg_2Si phase enhances the extrudability of the material [4]. The modeling of microsegregation and homogenization holding and cooling of 6xxx Al alloys and the mapping of phase fractions of Mg_2Si and β-AlFeSi versus alloy composition have been discussed in [5,6].

1.1. Effects of Chemical Composition

The main components of 6xxx alloys are silicon and magnesium, which allow age-hardening by coherent or semi-coherent Mg-Si precipitates. *Silicon* (0.3-1.2 wt. %) is responsible for high fluidity, low density and has very low solubility in Aluminum. It precipitates as virtually pure Si which is hard and improves the corrosion resistance. Also, it is observed that the ultimate tensile strength of Aluminum alloys is increased and the density of the alloys is decreased when silicon content is increased [17].

Magnesium (0.4-1.3 wt. %) increases the strength and hardness of the alloys, but in castings also decreases the ductility and impact resistance. The hardness and the tensile strength increase when magnesium content is increased. Furthermore, with increased amount of magnesium in the alloy, the average values of the Dendrite Arm Spacing and grain size reduced in cast condition [16].

With the addition of *Manganese* (0-0.8 wt. %), the 6xxx series Aluminum alloys enhance the strength simultaneously with increased ductility and contributes to uniform deformation. In the 6xxx series Aluminum alloys, the Mn-dispersoids formed during the homogenizing heat treatment behave as dislocated blocking particles and inhibit recrystallization after extrusion [18].

Iron (0-0.8 wt. %) is a common impurity in Aluminum alloys which can cause adverse effects to ductility and castability, particularly in Al-Si based casting alloys. Iron also plays a significant role in Aluminum solidification due to its strong tendency to partition. While normally presents as an impurity in small amounts around 0.2 wt%, iron tends to form intermetallic compounds with Aluminum and silicon, thereby affecting the solidification sequence and extrudability [19].

Chromium is added to Aluminum to control grain structure and for preventing grain growth in Al-Mg alloys and recrystallization in Al-Mg-Si alloys during heat treatment. Chromium also reduces stress corrosion susceptibility and improves toughness [20].

Zirconium is added to Aluminum to form a fine precipitate of intermetallic particles that inhibit crystallization [21].

The increase of *copper* content in an alloy also boosts the precipitation hardening through the stabilization of hardening phases like $Al_5Cu_2Mg_8Si_6$ and Al_2Cu. The increase of Si, Mg and Cu boosts the durability but reduces the extrudability [22].

1.2. Solidification

The metal solidifies after the casting process. The microstructure of the casting consists of three zones related to the size and morphology of the grains: the chill zone, the columnar zone and the equiaxed zone, as shown in *Figure 3*. In the *chill zone*, the liquid after its introduction into the mold cools abruptly at the points where it comes in contact with the cold wall of the mold and many small grains are formed. If the input temperature of the liquid in the mold is low, the liquid can be below the liquidus

temperature, so that the small crystals of the chill zone grow and new crystals are formed. Thus, the casting will have an equiaxed structure. On the contrary, if the input temperature is over liquidus temperature, only the crystals of chill zone are formed and create derdrites. This creates *columnar structure*.

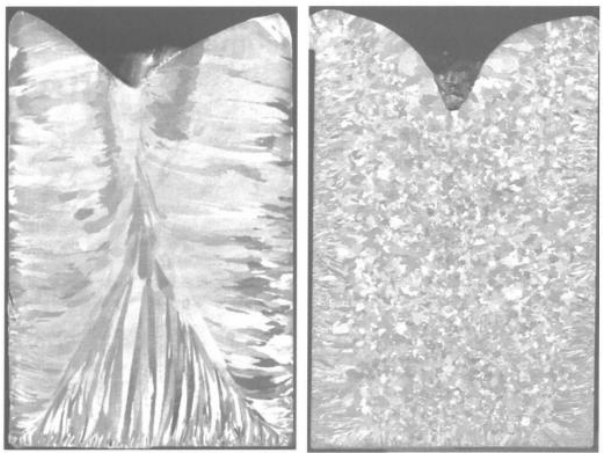

Figure 3: a) Al ingot exhibiting columnar structure, b) Al-3Si ingot showing chill, columnar and central equiaxed structure.

With the progress of solidification, the center of the cast is enriched with the second component causing constitutional supercooling. This situation leads to the nucleation of many new crystals, developed dendritic, but not directionally, thus giving the *equiaxed zone*. The formation of the equiaxed zone in the center of the cast is result of both the nucleation of new crystals and the multiplication of crystals. The solidification conditions affect the morphology of the dendritic structure and especially the Dendrite Arm Spacing, DAS. The lower the DAS is, the smaller the size of the grain is, which improves the mechanical properties. The microstructure described represents the as-cast morphology. This structure is modified by thermal treatments, which follow the casting. These treatments move the grain boundaries or activate various phase transformations to form the final microstructure.

The solidification of the billet results to modification of the composition from point to point, i.e. *segregation*. There are two different types of segregation, macro-segregation and microsegregation. The *microsegregation* is found in composition changes to the dendritic regions due to the rejection of the second component and is more important at the boundaries of the columnar zone. Microsegregation is a significant problem in castings, because it affects the mechanical properties, due to the heterogeneity in the distribution of the alloying elements in the grain scale. This problem is more important when thermal treatments follow the casting to strengthen the alloy. In the alloys Al-Mg-Si, the grains' inside lacks Mg, Si for the formation Mg_2Si during the process of precipitation.

The as-cast billets contain several inhomogeneities, such as elemental segregation, grain boundary segregation and formation of low-melting eutectics as well as the formation of iron intermetallics. The presence of intermetallic phases which have sharp edges, can affect the extrudability of 6xxx Al alloys especially when located in

the grain boundary regions. For the reasons above homogenization treatment is required.

1.3. Homogenization

Homogenization is the first process that an Aluminum alloy undergoes before it gets its final qualities. During homogenization, the alloy is heated in order to uniformly dissolve the alloying elements in matrix. At start, the alloy is being heat treated to high temperature, mostly ranging from 560 to 600^{o}C for a sufficient period of time, during which diffusion of alloying elements is activated from areas with high concentration to areas with low concentration. In this way the microstructure of Aluminum is transformed and especially, intermetallics diffuse from the grain boundaries in the inside into ultra-fine dispersion. This results in the elimination of the as-cast structure and the microsegregation, the spheroidization of intermetallic compounds and the transformation of β-to-α AlFeSi phase. At the same time, small particles of dispersoids precipitate in the center of the grain, consisting of α-Mn phase ($Al_{15}Si_4M_4$)

Key factors in homogenization process are:

- *Homogenization temperature*: is related to diffusion rate of alloying elements. Solid solution becomes more homogeneous the higher the temperature is, because alloying elements that diffuse into it increase.
- *Homogenization time*: in order to create a homogeneous solid solution it is important for homogenization time to be sufficient so that all alloying elements are completely diffused throughout the matrix.

Homogenization after casting of Aluminum alloys is an important process step which:

- Reduces microsegregation, leading to homogeneous properties across the secondary Dendrite Arm.
- Dissolves the eutectic phases formed during casting which have low melting point and may melt during subsequent processing.
- Helps in rounding of non-soluble phases to reduce stress concentrators, improving the fracture toughness and enhances surface finish.
- Facilitates precipitation of dispersoids which are on grain boundaries inhibiting recrystallization during extrusion (for alloys containing Mn, Cr, Zn and Sc). Non-recrystallized structure is preferred. Large crystallized grains reduce ductility and corrosion resistance and enhance enhance Precipitation Free Zones (PFZ) during aging.
- Eliminates the sharp structure of β-AlFeSi by the phase transformation β-to-αAlFeSi which results in a substantial increase in extrudability.
- Is mainly used on as cast parts and during its course, two main phase transformations take place:
    i. The β-AlFeSi to α-AlFeSi transformation.
    ii. Dissolution and re-precipitation of Mg_2Si.

Homogenization treatment for Aluminum alloys is aimed to modify the as-cast microstructure of the billet so that the extrudability is enhanced in terms extrusion pressure, extrusion speed, surface finish and mechanical properties of the final products. Homogenization treatment includes heating at a high temperature and a cooling step at some controlled rate. Extrudability is influenced by the amount of Mg, Si in solid solution and also from eutectic particles and Fe-bearing intermetallics, most important by β-AlFeSi. At first, the alloy is being heat treated to high temperature. Specific cycles vary, but actually for 6xxx alloys are performed 560-590^{o}C for 6-8 hours. According Mulazimoglou et al [7], the homogenization may be shortened by addition of elements such as Strontium (Sr) or Manganese (Mn), whereas for a fixed composition the temperature should increase. The addition of Strontium favors the formation of more desirable α-AlFeSi instead of platelike β-AlFeSi. Sr influences the Mg_2Si precipitation kinetics in 6xxx series Al alloys during solidification. Then the alloy part is cooled to room temperature. Cooling conditions determine the nature and amount of secondary phases precipitated, which influence parameters during thermal treatments that follow. These precipitates affect the age-hardenability of the alloy reducing the much desired mechanical strength of the alloy.

Specific topics of interest are the dissolution of Mg_2Si, the β-AlFeSi to α-AlFeSi transformation and the re-precipitation of Mg_2Si during homogenization cooling. Since Mg_2Si or Si particles dissolve rather fast, it is the β-to-α transformation kinetics which determines the minimum homogenization time.

1.3.1. The β-AlFeSi-to α AlFeSi transformation

During solidification Fe segregates to cell or dendrite arm boundaries where it takes part in eutectic reactions. It forms intermetallic phases with Al, Si and sometimes Mn. The AlFeSi intermetallic compounds play an important role in the microstructure of Aluminum alloys; influence the materials' properties during the following treatments and its surface quality.

The first and most important transformation during homogenization is the β-AlFeSi to α-AlFeSi (β-Al_9Fe_2Si and α-$Al_8(FeMn)_2Si$ respectively as the *Table 1* shows). The intermetallic compounds can form from the melt and from the supersaturated solid solution of the solidified Aluminum alloys. Fe has a very low solubility in the Al-matrix; almost all Fe will bind the excess Si and the Al to form Fe-containing intermetallics. During solidification, these intermetallics formed at the edge of the dendrites by a eutectic reaction, which explains their plate shape. Most of these intermetallics are the β-AlFeSi and a small fraction of the phases are the α-AlFeSi. These intermetallics do not dissolve and remain as separate phase in the Al-matrix even after long homogenization times, but they can change in phase composition and morphology.

Some authors comment on α-particles that nucleate at the beginning of the transformation on the boundary of β particles [8,9]. Birol et al [8] observed that the β particles are gradually replaced by uniform strings of cubic and hexagonal α-AlFeSi

particles. Sarafoglou et al [9] observed that β-particles break up into a necklace structure. They found that the individual particles in the intermediate homogenization state, exhibit partial transformation to the α-phase. The particles of the α-phase then coarsen and spheroidise at the expense of the remaining β-phase particles. The remaining α-particles coarsen when the homogenization process lasts longer than 10hours.

The β-AlFeSi, has a monoclinic structure and a plate-like morphology, which results in "pointy" and sharp microstructures that can cause cracking ruptures when extrusion is performed. On the contrary, α-AlFeSi has a cubic structure and a more rounded morphology, resembling a sphere. This morphology significantly reduces the cracking and produces an even surface, eliminating the defects of β-AlFeSi. The β-to-α AlFeSi phase transformation is claimed to increase extrudability [23]. Extrudability is defined by the maximum production speed for a given press capacity while still obtaining the desired mechanical properties, surface quality and geometric tolerances of the extrudate. The extrudability increases due to the β-to-α AlFeSi transformation and the parameter that quantifies the degree of β-to-α AlFeSi transformation is the ratio of the α-AlFeSi volume to the total volume of intermetallics. The increase of extrudability with the relative α fraction is caused by both improvement of the ductility and workability.

Table 1: Characteristics of α- and β-AlFeSi intermetallics

Property	**β**	**α**
shape	acicular [3,4,6,10,14] / plates [3,4,14]	Chinese script [3,6,10,12,14] / rod-like [4, 10]
aspect ratio	high	low
color	black [5,7,14]	gray [5,7,14]
stoichiometry	$Al_9Fe_2Si_2$ [8] Al_5FeSi [6,17]	$Al_{12}Fe_3Si_2$ [8,17] / Al_8Fe_2Si [6,17]
Fe:Si	1.0	1.5 / 2.0
crystal structure	monoclinic [11,13,14]	simple cubic, BCC [11,12,14] / HCP [9,13]
space group	A 2/a [16]	Im3 [11] / $P6_3/mmc$ [11]

All processes during homogenization are achieved by the diffusion of alloying elements through the matrix. The homogenization of iron intermetallics, mainly referring to α-AlFeSi and β-AlFeSi, can be separated into three stages according to Sarafoglou et al [9]. The alloy investigated was Al-0.38Mg-0.4Si-0.2Fe-0.03Mn (wt. %). Three homogenization heat treatments consisting of holding 560^{o}C for 2, 4, 6 hours followed by air cooling, in order to study the morphological changes of the α-AlFeSi phase after the complete transformation of β-to-α AlFeSi.

During the first stage, 2 hours of homogenization heating, the β-particles first get reduced to a necklace structure and then begin to become rounder, so that the

transformation to α-AlFeSi can be assumed completed. This is known as "Chinese script", is an as-cast morphology of mainly β-AlFeSi and it is eliminated during homogenization. Therefore, there are no β-AlFeSi particles after 2 hours. After the completion of the β-to-α AlFeSi, the intermetallic phase α-AlFeSi undergoes spheroidization. Firstly, the plate-like particles of α-AlFeSi exhibit a decrease in their width and then become more rounded at the edges [9].

On the second stage, 4 hours of homogenization process, pinching can be observed, i.e. the particles separate into smaller pieces and the edges of the particles keep getting rounder. Reduction in surface energy drives the rounding of edges.

On the final stage, 6 hours of homogenization process, the particles dissolve into small spheres and they line up and start to form necklace-like structures. This is caused by the reduction of the surface energy of the particles during the homogenization. The resulting α-particles are shorter, thicker and rod-like particles. The morphological changes of the α-AlFeSi described, include rounding of edges, pinching and spheroidization. The reduction of surface energy drives all the stages. Spherodization and in particular, necklace formation is a key process for increased extrudability. The morphological changes of the structure can be described by using certain sizes measurements such as feret and aspect ratio. These sizes get altered as the homogenization time goes by. Although they are a good representative of the structural transformations, they can only describe the change quantitatively [9].

The microstructural evolution of the 6060 Al-alloy during homogenization is depicted in *Figure 4*, the microstructural features of the as cast and as homogenized material are observed. More specifically in: (a) is depicted the as-cast microstructure, where it is observed Mg_2Si and intermetallics α, β-AlFeSi, which are located at the grain boundaries, while β-AlFeSi phase forms the characteristic 'Chinese-script' morphology. The morphological evolution with homogenization time is indicated in *Figure 4b* for 4 hours and *Figure* 4c for 6 hours homogenization time. Connectivity between intermetallics is decreased with homogenization time. Only after 6 hours of homogenization is observed clear spheroidization of particles and necklace formation.

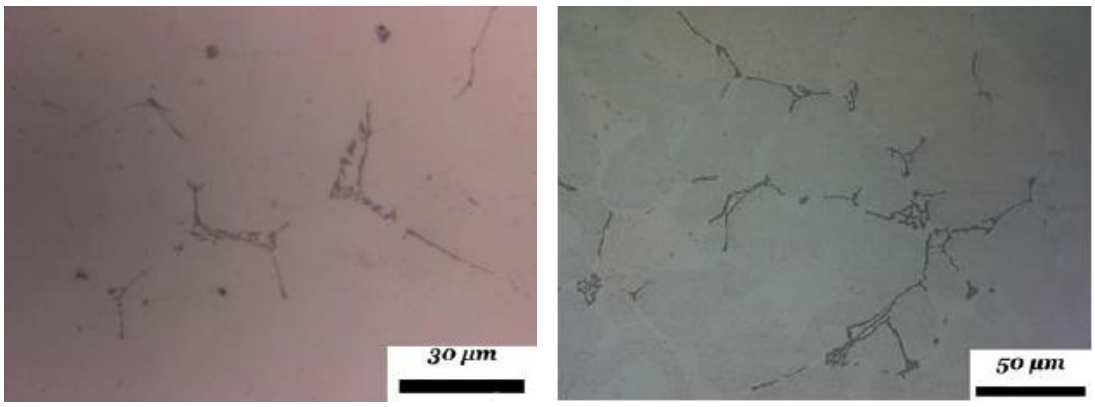

Figure 4: metallographic images of Alloy 6060: a) as-cast microstructure, homogenized at 560^{o}C b) for 4 hours and c) for 6 hours.

1.3.2. Dissolution and Re-precipitation of Mg_2Si

The second transformation during homogenization is the dissolution of Mg_2Si from the grain boundaries during the heating, and its re-precipitation during cooling to an even distribution throughout the body of the alloy with a more homogeneous in-grain distribution. The dissolution of Mg_2Si during homogenization is a fast process while the transformation of β-to-α-AlFeSi is a much slower process. In the as cast material, the particles of Mg_2Si are large, hard and with sharp edges and concentrated at the boundary of the grains. Larger Mg_2Si particles do not get dissolved. Instead, they coarse and grow in size, while the smaller ones are dissolved. The result is that while the total amount of particles depletes, their total surface area increases. This is called the Ostwald ripening effect or second phase coarsening. Through the first 2hours of homogenization, the smaller Mg_2Si precipitates are dissolved in the matrix. Mg_2Si precipitates during homogenization cooling, as the temperature drops below the solvus of Mg_2Si and coarsening of Mg_2Si grains begins.

Cooling after homogenization and its rate determines the precipitation behavior of Mg_2Si and thus influences extrusion performance of the billet and the final mechanical properties. During the homogenization cooling, the Mg_2Si phase re-precipitates and forms a new dispersion. The Particle Size Distribution (PSD) of this dispersion is an important parameter influencing extrudability. An increase is observed in both amount and size of Mg_2Si particles with a decreasing cooling rate. The hardness at room temperature and the flow stress at preheating temperature (450^{o}C) and extrusion temperature (500-550^{o}C) decrease with a slower cooling rate[24,26].

Large amounts of coarse β-Mg_2Si particles precipitate during a slow homogenization cooling rate. During extrusion, the undissolved β-Mg_2Si particles lead to incipient melting and surface defects. On the other hand, a fast cooled billet with fully solutionized Mg and Si is not desired, because it would lead to a rise in flow stress during extrusion, making the billet difficult to extrude. The microstructure desired is that the Mg_2Si particles mostly remain undissolved after preheating but become easily dissolved upon deformation. Therefore, it should be controlled the cooling rate during

homogenization. The precipitation of metastable β'-Mg_2Si phase instead of the equilibrium β-Mg_2Si phase, which is a result from some intermediate cooling rate, enhances the extrudability of the material. With step cooling at temperatures between 250-300^oC and with a cooling ratio between 100/200^oC/h, the Mg_2Si precipitates with the form of metastable β'-Mg_2Si, a fine precipitate with a small particle size [25].

To conclude with, homogenization is being done in order to increase the extrudability and strength of the alloy by the elimination of the as-cast morphology. While the β-AlFeSi to α-AlFeSi transformation plays a critical role to increasing extrudability, the dissolution and re-precipitation of Mg_2Si is one of the main strengthening factors of the alloy. The elimination of sharp and crack inducing β-AlFeSi particles in conjunction with the coarsening of Mg_2Si particles throughout the material body, results to a more extrudable and strong material. Those qualities are essential for a safe and successful application.

2. METHODOLOGY

Controlling the homogenization process is important in obtaining high extrudability and desirable properties in 6xxx Aluminum alloys. Computational thermodynamic and kinetic modeling is used for the description of microstructural evolution during solidification and homogenization, aiming at the improvement of the final properties of 6xxx Al-alloys. More specifically, the CALPHAD approach as implemented in the Thermo-Calc software was used to model thermodynamics and kinetics in multi-phase, multi-component systems[10,11,12]. Modeling of solidification and homogenization was performed on the 6060 Al-alloy with chemical composition given in the *Table 2*.

Table 2: Chemical Composition of 6060(%wt)

Mg	Si	Mn	Fe	Cu	Zn	Cr	Al
0.38	0.5	0.019	0.23	0.021	0.061	0.005	balanced

The present work deals with the modeling of solidification and cooling to room temperature, as well as the homogenization heating, holding and cooling. The processes investigated, the relevant phenomena and the models employed for the simulation are shown in *Table 3.* Segregation of elements and phases was treated with Scheil-Gulliver solidification model[13]. The dissolution of Mg_2Si and the transformation of β-AlFeSi to α-AlFeSi were treated with DICTRA based on multi-component diffusion in dispersed-phase systems[10,14]. All these modeling approaches are described in the next sections.

Table 3: Models used in the present work

Process	**Phenomena Modeled**	**Relevant Models**
Solidification	Microsegregation of elements and phases Nucleation and growth of intermetallics	Scheil-Gulliver Solidification Model
Homogenization (holding)	Transformation of β-to-α AlFeSi Dissolution of Mg_2Si	Multi-component diffusion with dispersed phases in an Al-matrix, in DICTRA

2.1. Thermodynamic Equilibrium Model

First of all, thermodynamic calculations were performed to determine phase stability in the system for the given chemical composition. Equilibrium calculations were treated using the Thermo-Calc software with the TCAL7 Al-alloy database. Thermodynamic calculations were performed on the provided chemical composition, to compute isopleth sections of the phase diagram, with respect to Si, Mg, Fe and Mn. Additionally, equilibrium calculations were performed to study the evolution of phase fractions with respect to temperature, at thermodynamic equilibrium, as well as to identify the liquidus and solidus temperatures, regarding solidification and solvus temperature of the intermetallic compounds in the system. The phases considered during the equilibrium calculations were:

- Liquid
- FCC_A1
- $Al_{13}Fe_4$
- Al_8Fe_2Si
- $Al_9Fe_2Si_2$
- $Al_{18}Fe_2Mg_7Si_{10}$
- Mg_2Si_C1
- $Al_{15}Si_2M_4$
- $Al_{15}Mn_3Si_2$
- Q_AlCuMgSi
- Diamond_A4

The FCC_A1 determines the α-(Al) Aluminum matrix phase. The Al_8Fe_2Si and $Al_9Fe_2Si_2$ phases are the Fe-bearing intermetallic phases. Especially, the Al_8Fe_2Si is known as α-AlFeSi and the $Al_9Fe_2Si_2$ is knows as β-AlFeSi. They are formed by eutectic reactions between Fe, Al, Si and sometimes Mn. The $Al_{13}Fe_4$ is an iron aluminide phase and it is known as Al_3Fe. The $Al_{18}Fe_2Mg_7Si_{10}$ is a quaternary stoichiometric intermetallic phase, known as π-, h- or φ- phase. The $Al_{15}Si_2M_4$ is an intermetallic phase originating from the Al-Mn-Si ternary system and commonly found in the form of cubic precipitates. The $Al_{15}Si_2M_4$ is also referred to as τ9. $Al_{15}Mn_3Si_2$ or α-Mn is rich in Fe and/or Mn, depending on the nominal alloy composition. The Q_AlCuMgSi is a quaternary Al-Cu-Mg-Si phase and it is known

as the Q-phase (not to be confused with the Fe containing q- or π phase) or $Al_5Cu_2Mg_8Si_6$ and commonly acts as a strengthening precipitate in Cu and Mg containing Aluminum alloys. The Diamond structure is pure Si. Some phases might not be observed in practice, even though they are stable, due to kinetic constraints. Especially, the formation of $Al_{13}Fe_4$ is hindered and substituted primarily by α-AlFeSi when Aluminum-Titanium Boride (AlTi5B) inoculation particles are used during casting.

2.2. Solidification Model

Solidification was treated by the Scheil-Gulliver model using the Thermo-Calc software with the TCAL7 Al-alloy database[13]. The Scheil-Gulliver model was used because of its accuracy for rapid solidification processes with minimal computational complexity. The model allows for the study of non-equilibrium solidification phenomena, including the development of elemental segregation at the level of the primary and secondary dendritic arms, the formation of non-equilibrium intermetallic phases and eutectic mixtures.

The following assumptions are made for the Scheil-Gulliver solidification simulation in Thermo-Calc:

- Diffusion in the liquid phase is assumed to be infinitely fast.
- Diffusion in the solid phases is slow enough to be ignored and as a result diffusion is assumed to be zero and what solidifies does not diffuse further.
- The liquid/solid interface is under thermodynamic equilibrium. Thus, the model better describes solidification under rapid cooling rates where diffusion in the solid can be neglected.

These assumptions are acceptable since the local solidification times encountered in industrial direct chill casting are short and the diffusion coefficient of the alloying elements in the liquid phase are significantly larger than those in the solid phase.

In the Scheil-Gulliver simulation the temperature is decreased step-by-step. When the temperature drops below the liquidus temperature the equilibrium amount and composition of solid and liquid phase is calculated. The solid phase is removed from the system and the amount and composition of the liquid phase is used for the next calculation step at a lower temperature. This procedure is repeated until the last liquid disappears. The outputs of Scheil-Gulliver calculations are the profiles of the intermetallic phases (wt. %) formed during solidification as well as the profiles of alloying elements in the FCC Al-matrix phase. These results represent the as-cast microstructure and were used as initial conditions for the homogenization simulations. Microsegregation in Aluminum alloys is a result of the low solubility of the alloying elements in the solid in relation with the liquid, which leads to the formation of secondary phases in the as-cast microstructure. The size and morphology of these phases depends on the chemical composition, the Dendrite Arm Spacing (DAS), the grain size and the local solidification time.

Assuming the diffusion is close to zero in the solid state during solidification, the composition profile of the alloying elements can be described with the Scheil equation:

$$C_s = C_o\, K\, (1 - f_s)^{K-1}$$

where C_o, the alloy nominal composition, K the partition coefficient and C_s the element composition when the solid weight fraction is f_s.

The phases considered during the Scheil-Gulliver calculations were less than the equilibrium phases in order to reduce computational complexity and these phases were:

- Liquid
- FCC_A1
- Al_8Fe_2Si
- $Al_9Fe_2Si_2$
- $Al_{18}Fe_2Mg_7Si_{10}$
- Mg_2Si_C1
- Diamond_A4

2.3. Homogenization Model

The homogenization heat treatment can be simulated as a diffusion-precipitation process. The phenomena that take place during homogenization are the removal of segregation, the phase dissolution and the precipitation inside the grains. The homogenization problem is separated computationally to the solidification cooling, homogenization heating, isothermal holding and homogenization cooling. During solidification cooling the intermetallics precipitate and then in homogenization heating they are dissolved. During isothermal holding it is observed the β-to-α AlFeSi transformation and during homogenization cooling Mg_2Si re-precipitates in small particle size. First of all, the simulation of the dissolution of Mg_2Si during homogenization and its re-precipitation during cooling was performed, though results might need to be reevaluated in a future study, using a Kampmann-Wagner (KWN) model to better describe the kinetics of nucleation, growth and dissolution of fine particles upon cooling [15]. Also, the simulation of the β-AlFeSi to α-AlFeSi was performed in DICTRA.

The required data for the homogenization simulation are:

- Initial concentration profiles of the alloying elements
- Secondary phase volume fractions
- Thermal cycle of homogenization
- A geometric model where the diffusion equations will be solved.

To study the evolution of the microstructure during homogenization treatment, multi-component, multi-phase diffusion simulations were performed in a system with dispersed phases in an FCC Al-matrix, using DICTRA module in Thermo-Calc with

the MOBAL5 Al-alloy database. A one-dimensional single cell planar geometry was employed in DICTRA, and the cell is selected to be 50μm, as shown in *Figure 6*. This cell is a result of the microstructure, where the grain size was measured about 100μm, as shown in *Figure 5*. The grain diameter is 100μm, remaining constant after the homogenization treatment. Due to symmetry, only half of the grain was simulated, from the boundary to the center of the grain. Thus, diffusion was solved in a 50μm diffusion cell with an FCC Al-matrix structure, while the secondary phases are considered as dispersed phases in the matrix. The elements used for the homogenization simulations in DICTRA were, Al, Mg, Si, Fe and Mn, the weight percent of which were reported in *Table 2* and the phases considered were:

- FCC_A1
- Al_8Fe_2Si
- $Al_9Fe_2Si_2$
- $Al_{18}Fe_2Mg_7Si_{10}$
- Mg_2Si_C1
- Diamond_A4

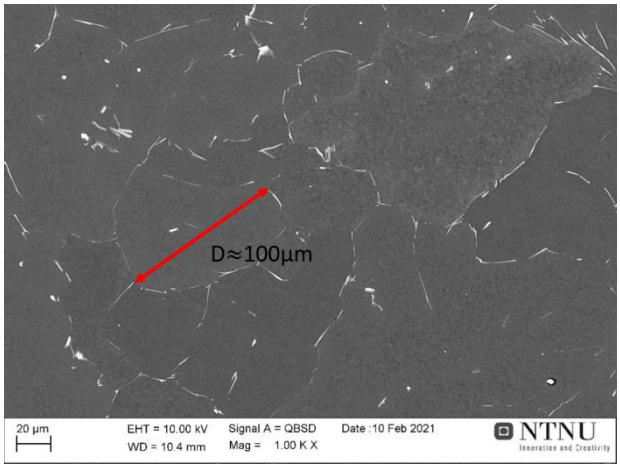

Figure 5: Microstructure as-cast of 6060 Aluminum alloy.

The dissolution of Mg_2Si and the transformation of β-AlFeSi to α-AlFeSi during homogenization are treated with multi-component, multi-phase diffusion simulations in dispersed-phase systems. Diffusion is assumed to take place only in the matrix phase and according to the dispersed model in DICTRA. The Dispersed Phase Model in DICTRA treats problem involving diffusion through microstructures containing dispersed precipitates or secondary phases. The dispersed phases are considered as "non-diffusion phases" and they act as point sinks or sources of solute atoms (alloying elements). The matrix diffusion controls the overall kinetics, because the growth and dissolution rates of dispersed phases are very high compared with the rates in the matrix. This assumption is tolerable for the high homogenization temperatures, since the growth-dissolution rates are very high and the particles reach the equilibrium state very fast.

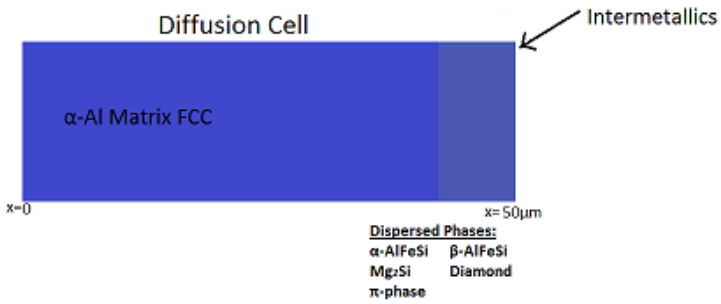

Figure 6: Diffusion Cell for homogenization simulation.

The volume fraction of the phases and the segregation profiles of the elements in the phases (wt. %) obtained by the Scheil-Gulliver model, were used as input for the kinetic calculations in DICTRA. The Scheil-Gulliver segregation profiles represent the as-cast microstructure. To the end, the fraction solid f_s, derived from Scheil was converted to a distance axis via the relation:

$$x_s = f_s\, L \qquad (1)$$

where L is the length of the diffusion cell, 50μm. The initial phase fraction of the intermetallic phases, required for the diffusion simulations, was obtained by differentiating the phase profiles obtained by Scheil-Gulliver simulations with respect to the diffusion distance. Thus the diffusion problem was solved in one dimension. The phase transformations that were treated in the diffusion cell are the Mg_2Si, the π-phase ($Al_{18}Fe_2Mg_7Si_{10}$) and pure Si (Diamond) dissolution as well as the β-to-α AlFeSi transformation. Both are diffusional transformations and their rate is controlled by the diffusion of alloying elements. Grain boundary diffusion was not considered, as during homogenization process, diffusion takes place from the boundaries, where is the end of the solidification, to the grain interiors in order to eliminate the microsegregation gradients. The volume fraction of dispersed phases is calculated from the local composition in each node, assuming local equilibrium. The growth or dissolution of phases leads to adjustments in the concentration profiles of the elements to be used in the next time-step of the calculation. Thus, in each step change the volume fraction of phases and the local composition profiles through the matrix diffusion. The solution of the diffusion equation is performed under the following boundary and initial conditions. Considering a closed system, the boundary conditions are:

$$J_i(0,t) = J_i(L,t) = 0 \qquad (2)$$

where J_i are the elemental fluxes with i=Mn, Mg, Si, Fe. In terms of concentration gradients, the above equation becomes:

$$\frac{\partial c_i}{\partial x} = 0 \; for \; x = 0 \; and \; x = L \quad (3)$$

The initial conditions for the diffusion problem are the result of the Scheil-Gulliver calculations, converted over the diffusion distance using equation (1), for *t=0* and can be expressed as follows for the elements:

$$c_i(x,0) = c_i^s(x) \qquad (4)$$

while for the phases:

$$f_k(x,0) = \frac{\partial f_k^s}{\partial f_s} \rightarrow \frac{1}{L}\int_0^x f_k(s,0)ds = f_k^s(f_s(x)) \quad (5)$$

where *k*= Mg_2Si, α-AlFeSi, β-AlFeSi, Si (Diamond), π-phase and $c_i^s(x)$ and $f_k^s(x)$ are the composition profiles and phase fractions, resulting from the Scheil-Gulliver simulation.

In DICTRA, the diffusivities are products of mobilities and corresponding thermodynamic factors. The mobility paremeter, M_i for an element in a given phase is described by a frequency factor M_i^0 and activation energy ΔG_i^*, which are related by the following equation:

$$M_i = \frac{M_i^0}{RT} exp\left(-\frac{\Delta G_i^*}{RT}\right) \qquad (6)$$

where R is the gas constant and T is the absolute temperature. Both M_i^0 and ΔG_i^* are composition dependent.

The thermal cycle is an operational parameter for the homogenization simulation. To calculate the evolution of the temperature during solidification cooling, a one-dimensional radial heat transfer simulation was employed. Temperature measurements were not available for this stage and heat transfer simulations were used to approximate it. The calculated cooling curve was then used in the diffusion simulations to calculate the evolution of the microstructure during solidification. An explicit finite difference scheme was applied in a MATLAB script to solve the heat equations in a cylindrical geometry, because the billets are cylindrical and temperature and composition depend on thermophysical properties. The thermophysical properties are composition and temperature dependent. Thermo-Calc was used to calculate the thermophysical properties as a function of composition and temperature, during the numerical integration of the heat transfer equation.

$$\frac{1}{r}\frac{\partial}{\partial r}\left(k\, r\, \frac{\partial T}{\partial r}\right) = \rho\, c_p \frac{\partial T}{\partial t}$$

Where, ρ represents the density(kg/m^3), c_p the heat capacity (J/K) and k the thermal conductivity (W/mK) and they depend from temperature. The boundary conditions for this problem are:

$$r = 0 \rightarrow\ q = -k\frac{dT}{dr} = 0\ (because\ of\ sumetry)$$

where q represents the heat flux (W/m^2).

r=R→T=20°C (because the surface is in contact with water)

The numerical solution of the radial heat transfer problem allows the determination of the temperature history as a function of the billet radius. In order to perform calculations of the microstructural evolution during solidification cooling in DICTRA, a reference temperature history at 2/3 of the outer billet radius was used. An analytical equation was fitted to the numerical data in order to provide the appropriate DICTRA input as follows:

$$T = a\,exp(-bt) + c \qquad {}^{o}C$$

where α*=757.8°C, b=0.05107s*$^{-1}$ and *c=25.17°C.*

Results regarding the temperature profile as a function of the billet radius at different times, as well as the temperature history at selected radii, are presented in *Figures 7a and b.*

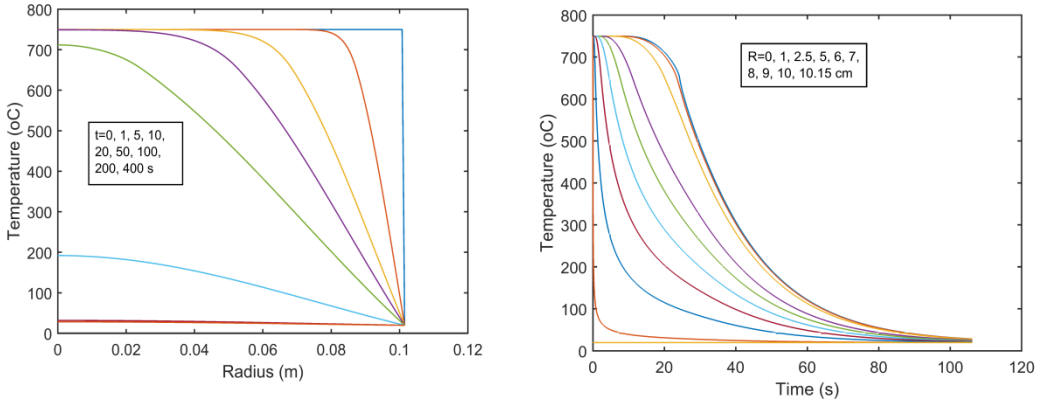

a) b)

Figure 7: Temperature field upon solidification cooling, according to heat transfer simulations, a) Temperature profiles as a function of radius at different times and b) the temperature variation with time at selected radii.

For the homogenization heating and holding, the temperature measurements were provided by the industry and fitted to the problem resulting:

$$T = a\,(1 - \exp(-bt))^{c} \quad {}^{o}C$$

Where α is the homogenization holding temperature, i.e. the maximum temperature observed during homogenization process, equal to *570°C*, *b=2.1161*10*$^{-4}$*s*$^{-1}$ and *c=1.748399 (dimensionless).*

The transfer problem results in the evolution of the temperature field along the billet, providing input for DICTRA.

Concluding, the profiles of alloying elements and the volume fractions of the intermetallic phases, provided by the Scheil-Gulliver Solidification Model, and the thermal cycle are used as inputs for the simulation of the homogenization process to the diffusion cell described above. To study the evolution of the microstructure during

homogenization treatment, multi-component, multi-phase diffusion simulations were performed in a system with dispersed phases in an FCC Al-matrix.

It should be emphasized that although, the methodology described has been used successfully in the past by Sarafoglou et al [6,9] to model and optimize the heat treatment process of Al-alloys, experimental calibration and validation is required. Characterization of the phases present after solidification and homogenization is required to provide feedback for the model development.

3. RESULTS

3.1. Thermodynamics

Thermodynamic calculations were performed on the provided chemical composition (as shown in *Table 2)* in order to determine phase stability. The volume fraction of phases present at thermodynamic equilibrium was calculated as a function of temperature, considering all stable phases involved in the alloying system, as shown in *Figure 8*. In high temperatures, the material is liquid. As the temperature decreases, equilibrium solidification starts at the liquidus temperature, $T_{liquidus}=654.5^oC$ with the precipitation of the Aluminum FCC matrix, from the liquid. Subsequent cooling results in the precipitation of $Al_{13}Fe_4$ phase (known as Al_3Fe) in $T=633.6^oC$, from the liquid, as solidification progresses. The $Al_{13}Fe_4$ phase becomes unstable at $T=621.3^oC$ and is replaced by the Al_8Fe_2Si intermetallic compound (known as α-AlFeSi). The end of solidification, denoted by the complete consumption of the liquid phases, takes place at the equilibrium solidus temperature, $T_{solidus}=618.3^oC$. Further cooling results in a minimal increase of the Al_8Fe_2Si volume fraction followed by its decrease, as the $Al_9Fe_2Si_2$ intermetallic compound (known as β-AlFeSi) begins to grow in $T_{sol\_\beta\text{-}AlFeSi}=573.3^oC$.The solvus temperature of $Al_9Fe_2Si_2$ is very close to the nominal homogenization temperature $T_{homogenization}=580^oC$ and above the actual achievable homogenization temperature, measured to be 570^oC. The volume fraction of Al_8Fe_2Si decreases with the drop of temperature until $T_{sol\_\alpha\text{-}AlFeSi}=566.5^oC$, indicating the complete dissolution of α-AlFeSi. Then, in $T=449.7^oC$ precipitates the $Al_{18}Fe_2Mg_7Si_{10}$ (π-phase) and at lower temperatures, the $Al_{15}Si_2M_4$ intermetallic (τ9 phase) appears. At 210°C, the Q_AlCuMgSi (Q-phase) becomes thermodynamically stable. The final stable phase is pure Si with a Diamond structure, appearing below 200°C. The Diamond phase instantly consumes the $Al_{18}Fe_2Mg_7Si_{10}$ and promotes the formation of Mg_2Si and $Al_9Fe_2Si_2$ intermetallic compounds.

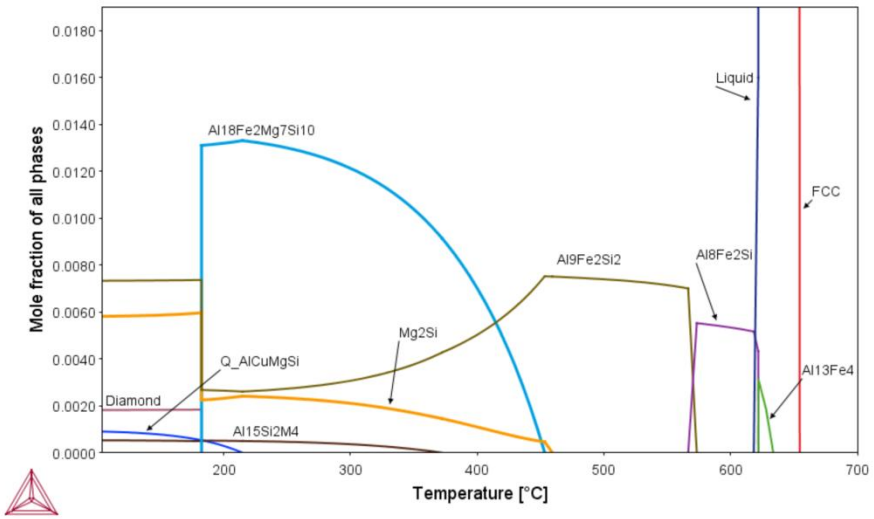

Figure 8: Evolution of equilibrium volume fraction of phases for the 6060 Al-alloy.

To determine the effect of composition on the phase transition temperatures during solidification and homogenization, isopleth sections of the phase diagram were computed with respect to Mg, Si, Fe and Mn, varying one alloying element at a time and maintaining the nominal constant concentration for the other elements. The isopleth sections were computed as a function of composition and temperature in the range of 0 to 1wt% for every alloying element. To simplify the calculation, only the Al_8Fe_2Si (α-AlFeSi), $Al_9Fe_2Si_2$ (β-AlFeSi), $Al_{18}Fe_2Mg_7Si_{10}$ (π-phase), Diamond (Si), Mg_2Si, liquid and FCC Al-matrix were considered in the phase diagram, as shown in *Figure 9*. The solidus, liquidus and solvus temperature of intermetallic phases are affected by composition. The liquidus and solidus temperature, i.e. the temperatures that correspond to the initiation and ending of equilibrium solidification decrease by the addition of Mg, Si and Mn and increase by the addition of Fe. With the exception of Si, the variation of the liquidus and solidus temperatures is limited in the examined composition range. As shown in *Figure 9a*, the solvus of α-AlFeSi and β-AlFeSi, i.e. the temperature that the phase is completely dissolved, are remain relatively constant by the addition of Mg. The addition of Si and Mn, promotes the formation of β-AlFeSi at elevated temperatures, as both solvus temperatures increase. The addition of Fe promotes the formation of α-AlFeSi against β-AlFeSi at elevated temperatures, as both solvus temperatures decrease. According to thermodynamics, the range of stability of α-AlFeSi and β-AlFeSi is dependent on the Si, Fe and Mn content of the alloy and most importantly on the ratio of Fe/Si and Mn/Si. Excess Si and Mn can promote β-AlFeSi, requiring higher homogenization temperatures to complete the β-to-α AlFeSi transformation.

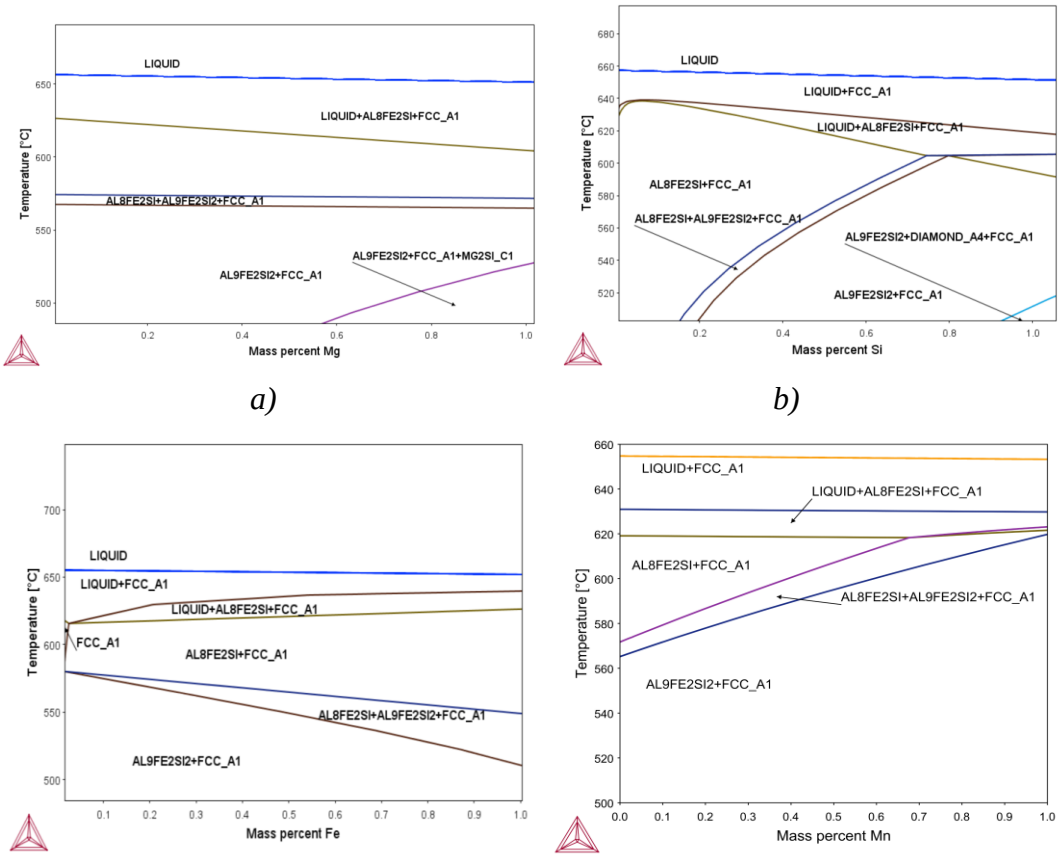

Figure 9: Isopleth sections of the phase diagrams for the 6060 Al-alloy, with respect to a) Mg, b) Si, c) Fe and d) Mn, near the solidification and homogenization temperature range.

3.2. Solidification

Solidification was modeled using Scheil-Gulliver approach. To ease computational complexity, were considered only the major alloying elements, including Si, Mg, Mn and Fe and the phases, FCC Al-matrix, Al_8Fe_2Si (α-AlFeSi), $Al_9Fe_2Si_2$ (β-AlFeSi), Mg_2Si and Diamond (Si) in the solidification and homogenization calculations.

The solidification path, the evolution of phase fractions and the development of elemental segregation at grain boundaries are presented in *Figure 9*. The solidification sequence is depicted in *Figure 10a*, with respect to temperature and mass fraction of solid. The phase sequence during solidification is:

FCC Al-matrix→Al_8Fe_2Si (α-AlFeSi)→$Al_9Fe_2Si_2$ (β-AlFeSi)→Mg_2Si→Diamond (Si)

The evolution of the phase fractions as a function of temperature is shown in *Figure 10b*. Solidification begins at the thermodynamic equilibrium liquidus temperature, $T_{liquidus}=654.5^oC$, with the nucleation and growth of α-Al FCC dendrites. At 625^oC, the Al_8Fe_2Si (α-AlFeSi) nucleates and grows with the α-Al matrix. The growth of Al_8Fe_2Si (α-AlFeSi) stops at approximately 598^oC, where the $Al_9Fe_2Si_2$ (β-AlFeSi) begins to grow with the α-Al matrix, until the consumption of the liquid. As the temperature decreases, the Mg_2Si nucleates at 568^oC and grows along with the β-

AlFeSi and α-Al matrix. Finally, the Diamond (Si) becomes stable at 557^oC and the rest of liquid solidifies rapidly to a eutectic mixture of Diamond (Si), Mg_2Si, β-AlFeSi and α-Al. That temperature constitutes the non-equilibrium solidus temperature, $T_{solidus}=557^oC$, where solidification is complete. The secondary phases were formed near the grain boundaries.

During a second iteration of calculations, the $Al_{18}Fe_2Mg_7Si_{10}$ (π-phase) was added to the Scheil-Gulliver model, since significant fractions of π-phase were observed experimentally after solidification cooling. The solidification path, the evolution of phase fractions and the development of elemental segregation at grain boundaries are presented in *Figure 12*. The solidification sequence is depicted in *Figure 12a*, with respect to temperature and mass fraction of solid. The phase sequence during solidification is:

FCC Al-matrix→ Al_8Fe_2Si(α-AlFeSi)→ $Al_9Fe_2Si_2$(β-AlFeSi)→Mg_2Si→$Al_{18}Fe_2Mg_7Si_{10}$→ Diamond

The evolution of phase fractions is as mentioned above with the difference that at $T=560^oC$ the $Al_{18}Fe_2Mg_7Si_{10}$ (π-phase) nucleates and grow, until its consumption from Diamond (Si) at $T=557^oC$.

The Scheil-Gulliver solidification model predicts an increased freezing range (the difference between the liquidus and solidus temperature), compared to the equilibrium solidification model. According to equilibrium calculations, the freezing range is 36.2^oC, whereas in the Scheil calculations, the freezing range is 97.5^oC. This difference is due to the development of elemental segregation at the level of the primary and secondary dendritic arms, due to the high cooling rates exist during solidification. The Scheil-Gulliver model predicts the composition of intermetallic phases. The profiles of the alloying elements in the matrix are shown in *Figure 11*, where microsegregation appears. Mg concentration drops close to grain boundary due to the formation of Mg_2Si and Fe drops due to the formation of iron intermetallics, α-AlFeSi and β-AlFeSi. The Scheil-Gulliver calculations provide the initial conditions for the homogenization simulation. The solidification model should be validated experimentally.

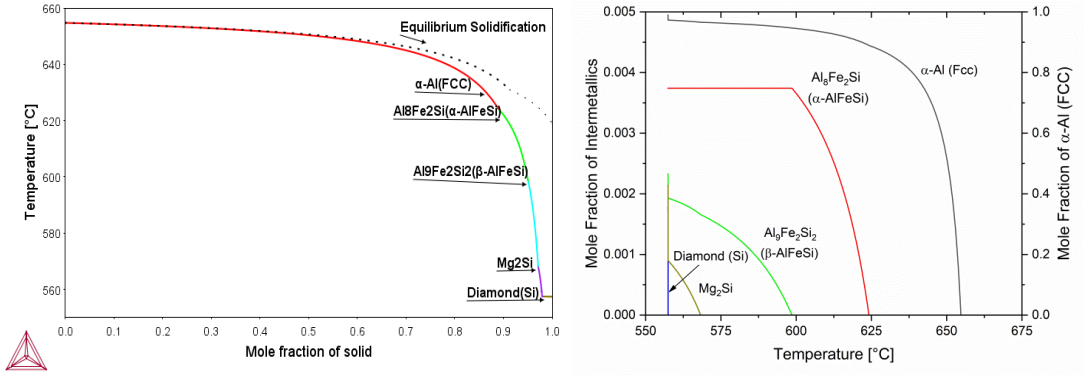

a) *b)*

Figure 10: Scheil-Gulliver solidification results, regarding a) the solidification path, i.e. the temperature as a function of the solid fraction and b) the phase fractions as a fraction of temperature.

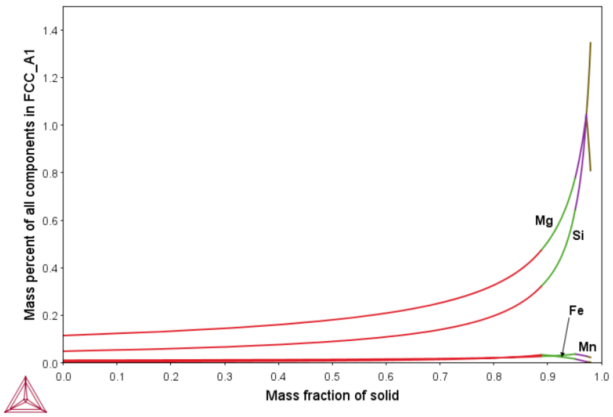

Figure 11: Profiles of alloying elements in the Al- matrix (FCC) after solidification.

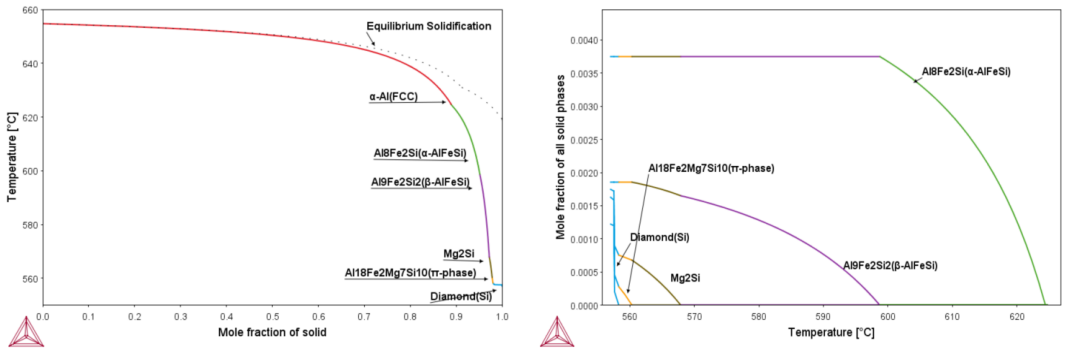

a) *b)*

Figure 12: Scheil-Gulliver solidification results, including $Al_{18}Fe_2Mg_7Si_{10}$ (π-phase), regarding a) the solidification path, i.e. the temperature as a function of the solid fraction and b) the phase fractions as a fraction of temperature.

3.3. Homogenization

Multi-phase, multi-component diffusion simulations were employed in DICTRA, to calculate the homogenization of the as-cast material, the degree of elimination of elemental segregation, the dissolution of intermetallic phases and eutectic mixtures and the transformation of β-to-α AlFeSi. Firstly, only the α-Al (FCC), Al_8Fe_2Si (α-AlFeSi), $Al_9Fe_2Si_2$ (β-AlFeSi), Mg_2Si and Diamond (Si) intermetallic phases were considered during diffusion calculations. The selection of phases involved in the calculations should be validated experimentally and model adjustments should be made accordingly.

Results regarding the evolution of phase fractions and the composition of the α-Al matrix, during solidification cooling and homogenization heating, holding and cooling are shown in *Figure 13*. The local phase fractions of intermetallic phases as a function of distance in the diffusion cell, at selected times are presented in *Figure 14*. The local chemical composition of the α-Al matrix, indicating the degree of segregation, is given as a function of distance in the diffusion cell, at selected times, as depicted in

Figure 15. The right side of the diffusion cell corresponds to the center of the primary dendrite, whereas the left side represents the end of the dendrite arm, near the grain boundary, where the last liquid was solidifies. Results from Scheil-Gulliver simulations were used to obtain the initial phase fractions and compositions, as shown in *Figures 14a, 15a*. The intermetallic phases formed near the grain boundary where the liquid solidifies at the lowest temperature. A mixture of intermetallic phases is found in the right side of the diffusion cell, according to the solidification sequence:
FCC Al-matrix → Al_8Fe_2Si (α-AlFeSi) →$Al_9Fe_2Si_2$ (β-AlFeSi) → Mg_2Si → Diamond (Si)

After solidification, the segregation of alloying elements near the grain boundaries is depicted in *Figure 15a*, where Si and Mg concentrations in the Al-matrix reach a value of 1.35% and 1.05%wt, respectively.

During cooling to room temperature after solidification, according to the temperature curve, given in *Figure 13a*, the volume fraction of Al_8Fe_2Si (α-AlFeSi) decreases significantly, whereas the volume fractions of Mg_2Si, β-AlFeSi and Diamond (Si) increase. The α-AlFeSi dissolves completely and re-precipitates and grows at late stages of homogenization. As the function of intermetallic compounds increase during cooling and oversaturation of alloying elements decreases, as shown in *Figures 13c, d*, thus, the segregation profiles of the α-Al matrix decrease. It should be noted that the predicted phase fractions at the end of cooling might be lower and supersaturation of the α-Al matrix higher in practice because the model might overestimate the formation kinetics of intermetallic compound under rapid cooling rate.

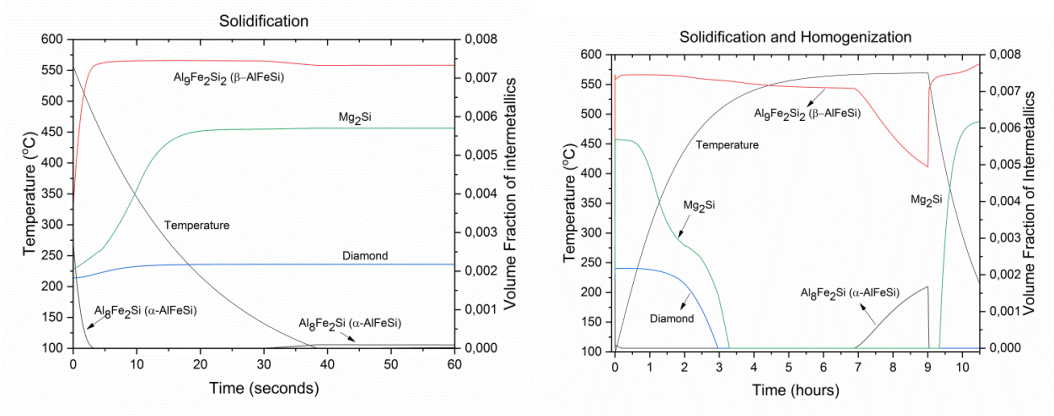

a) *b)*

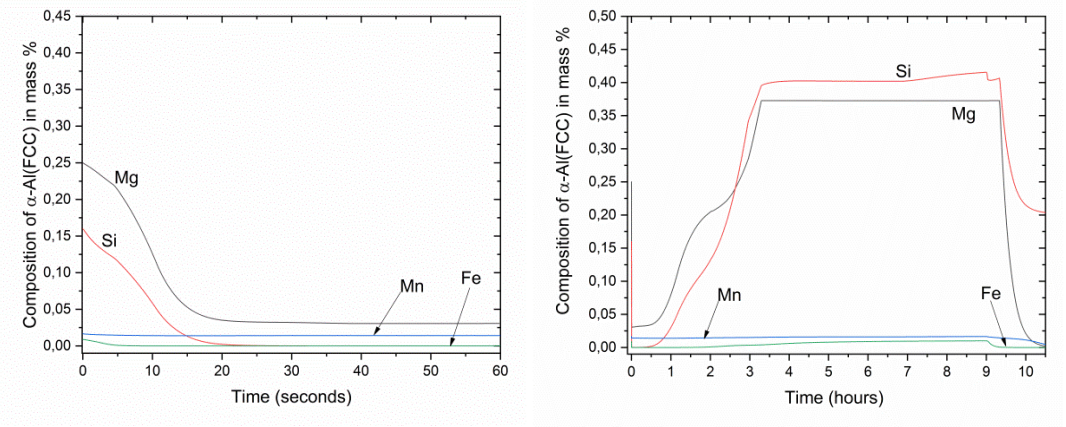

c) *d)*

Figure 13: Evolution of a) phase fractions during solidification cooling, b) phase fractions during homogenization, c) composition of the α-Al matrix during solidification, d) composition of the Al-matrix during homogenization.

During homogenization heating, the small fraction of Al_8Fe_2Si (α-AlFeSi) dissolves rapidly, while the fraction of $Al_9Fe_2Si_2$ (β-AlFeSi), Mg_2Si and Diamond (Si) slowly decreases, because in low temperatures diffusion is sluggish, as shown in *Figure 13b*. As intermetallic phases dissolve, alloying elements are released in the matrix and the concentration of Al-matrix increases, as shown in *Figure 13d*. By the increase of temperature, the eutectic mixture, containing β-AlFeSi, Mg_2Si and Diamond (Si), decreases in fraction and after 3 hours of homogenization process the Diamond (Si) is eliminated. The Mg_2Si are initially spheroidized and later dissolved completely at 3.4 hours of treatment, as depicted in *Figure 13c*, *14c-14e*. The dissolution of Mg_2Si and Diamond (Si), results in the exaggeration of segregation profiles, because alloying elements are released in the matrix, as depicted in *Figures 15c*, *d*. As the Mg_2Si and Diamond (Si) are eliminated, the release of Mg and Si stop, forming a plateau in the composition of the α-Al matrix, as shown in *Figure 13d*. During homogenization, as the temperature increases, the segregation of alloying elements is eliminated, because they diffuse in the matrix and composition becomes homogeneous, as shown in *Figures 15e-g*.

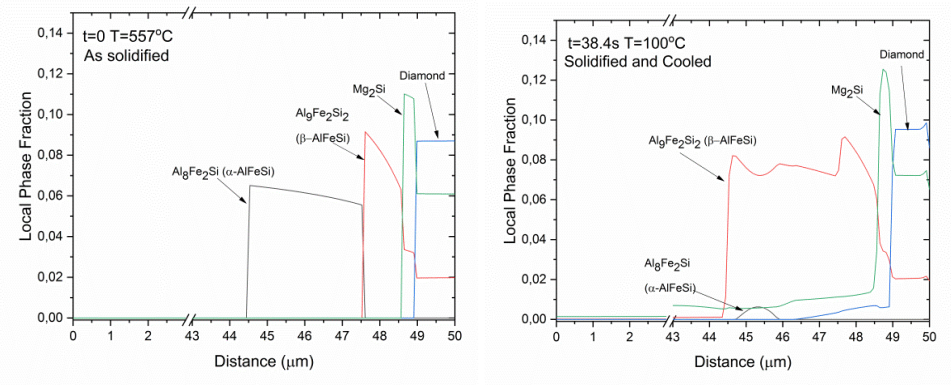

a) *b)*

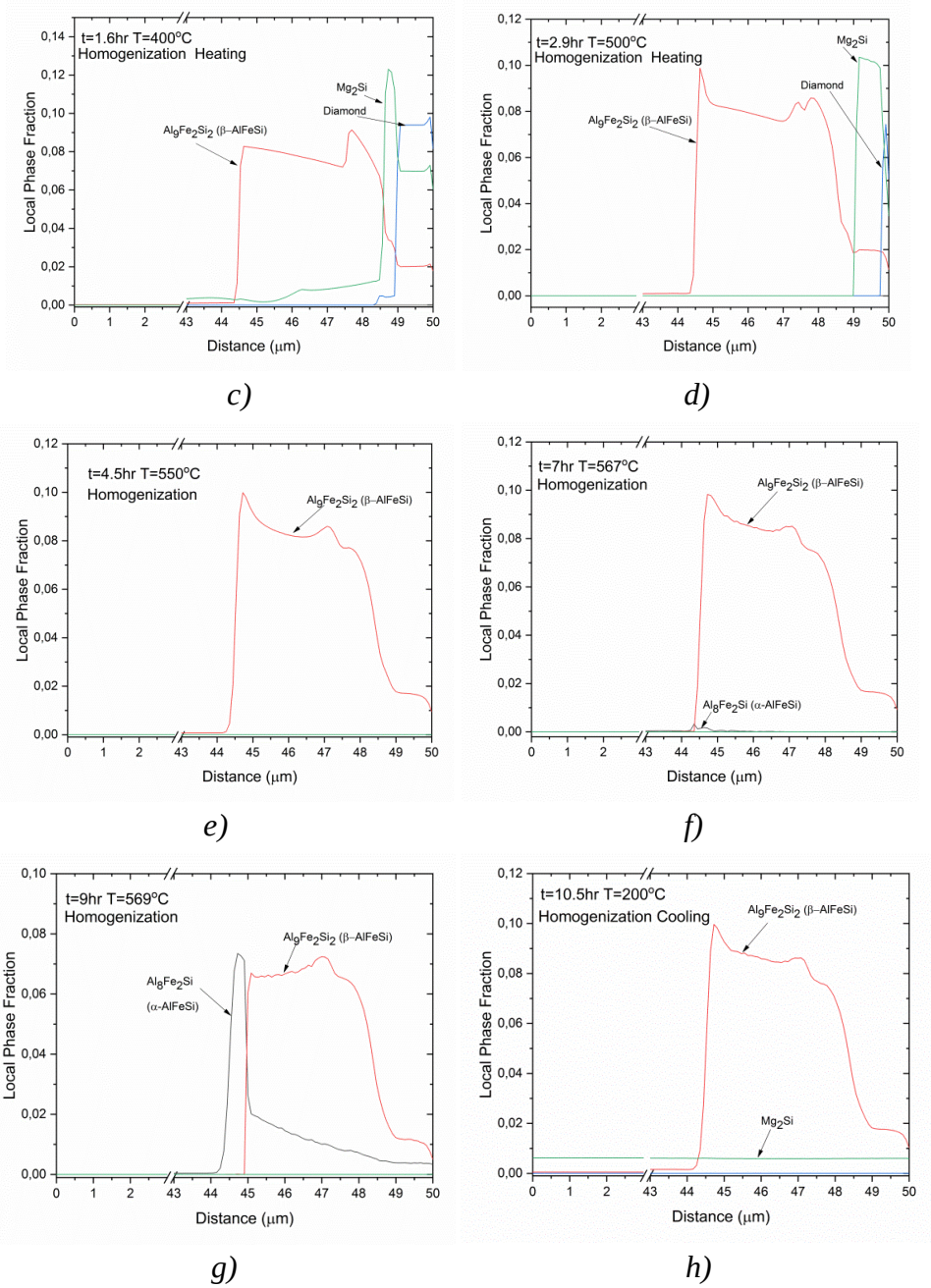

Figure 14: Local intermetallic phase fractions as a function of distance in the diffusion cell, at various times during homogenization treatment. The right side of the cell corresponds to the center of the primary dendrite, whereas the left side to grain boundary.

After the dissolution of the Mg_2Si and Diamond (Si), the β-AlFeSi remains the main intermetallic compound, with a minimal decrease in phase fraction during homogenization heating and holding, as shown in *Figures 14e,f.* During homogenization holding, the composition of α-Al matrix remains relatively constant, as shown in *Figures 15e, f.* At 7 hours of homogenization process, the α-AlFeSi nucleates together with the β-AlFeSi and begins to grow as the temperature increases, as the β-to-α transformation is favored. During homogenization holding at temperature approximately 570°C, the α-AlFeSi grows against the β-AlFeSi, as

depicted in *Figure 14g*, while the composition of α-Al matrix remains stable, as shown in *Figure 15g*.

During homogenization cooling, after 9 hours of treatment, the temperature decreases rapidly and the reverse transformation of α-to-β AlFeSi observed, as the β-AlFeSi grows against the α-AlFeSi, until the complete consumption of the later, as shown in *Figures 13b and 14h*. Additionally, the Mg_2Si particles re-precipitate, when the solvus temperature of Mg_2Si is reached, as shown in *Figures 13b and 14h*, and the phases grow rapidly, decreasing the concentration of alloying elements in α-Al matrix, as shown in *Figures 13d and 15h*. The local phase fractions and composition profiles at the end of homogenization cooling are depicted in *Figures 14h and 15h*, where homogeneous dispersion of Mg_2Si particles has formed and β-AlFeSi particles remain near the boundary.

The results regarding the homogenization cooling must be interpreted with care, because the present model overestimates the transformation rates of α-to-β AlFeSi and the precipitation kinetics of Mg_2Si under rapid cooling rates. The homogenization cooling can be simulated using PRISMA, which is not included in this project.

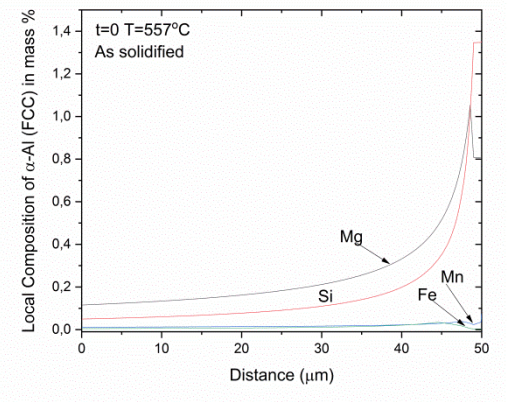

a)

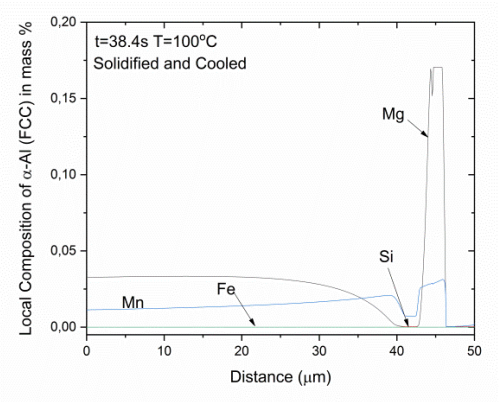

b)

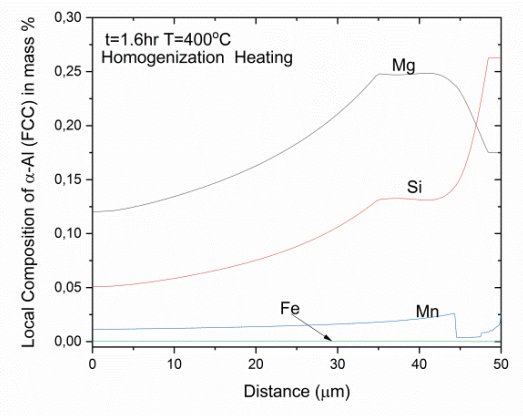

c)

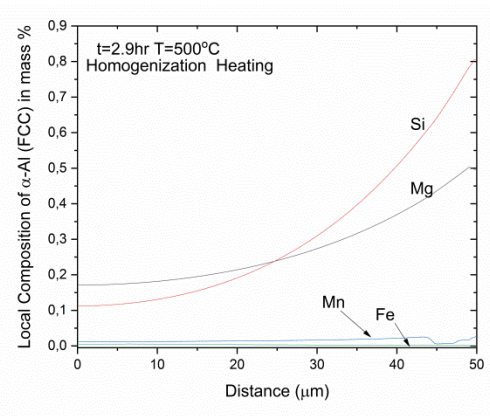

d)

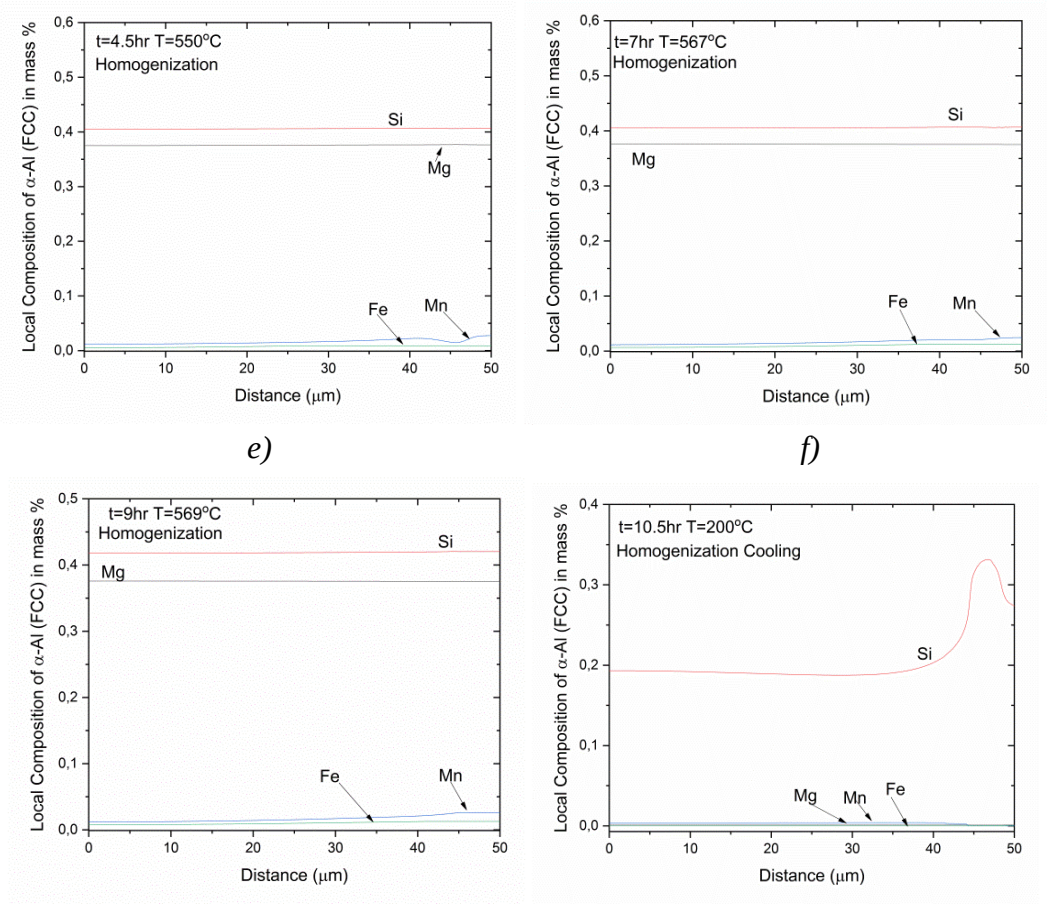

Figure 15: Local composition of the α-Al matrix as a function of distance in the diffusion cell, at various times during homogenization treatment. The right side of the cell corresponds to the center of the primary dendrite, whereas the left side to grain boundary.

3.4. Experimental Validation

The validity of the simulation results were confirmed via experimental measurements. Characterization of the received material from the industry was performed for the as-cast and homogenized Al-alloy microstructure. The characterization of the as-cast material was performed by SINTEF, using Scanning Electron Microscopy (SEM), Energy Dispersive X-Ray point analysis (EDX) and image analysis. Metallographic analysis of the as-cast material, using Light Optical Microscopy was performed at the Laboratory of Materials at the University of Thessaly. Samples from the center, middle and edge of the billet along the radius, as shown in *Figure 16*, were analyzed to determine the fraction and morphology of the intermetallic phases that exist and the composition of these phases, after casting and cooling.

Figure 16: As-cast Al-alloy 6060, sections of received as-cast for the characterization analysis.

The microstructure of the as-cast material via Light Optical Microscopy at the billet center, middle and edge are shown in *Figures 17, 18 and 19*, respectively. Metallographic images are presented at three different magnification levels, x100, x200 and x500. No significant variations along the billet radius were observed, as shown in *Figures 17, 18 and 19.* After solidification and cooling, intermetallic compounds exist in grain boundaries and in between the secondary dendritic arms. Most of the particles have rod shaped morphology, typical of β-AlFeSi, which limits extrudability. Also, are presented some rounded particles and eutectic mixtures. The intermetallics in between dendritic arms and near grain boundaries are result of elemental segregation in those areas, because of rapid cooling rate during casting. Optical Microscopy cannot be used to identify the phases and are used SEM and EDX analysis, to determine the structure and the volume fractions of the intermetallic phases.

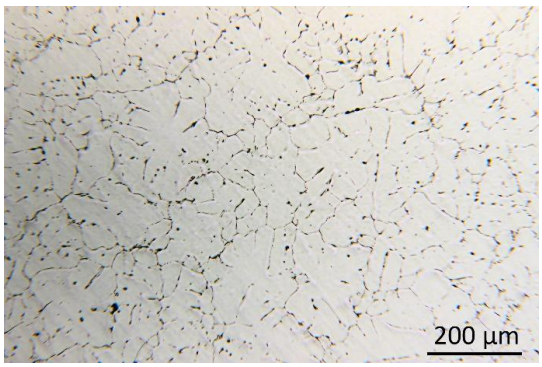

a)

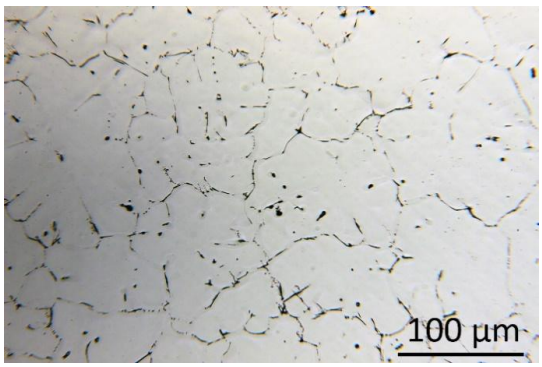

b)

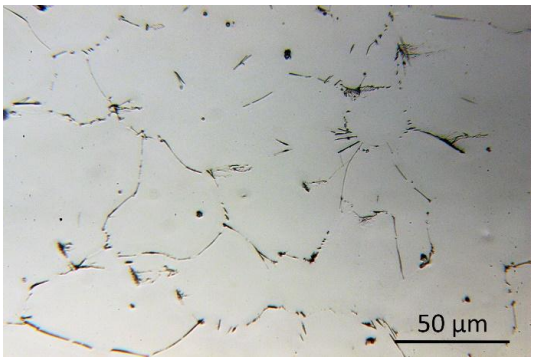

c)

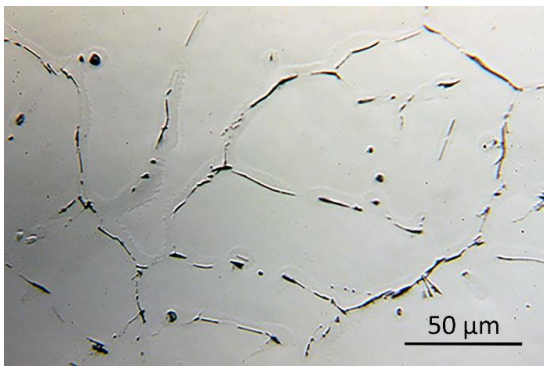

d)

Figure 17: Metallography of as-cast Al-alloy 6060, center section. Magnification: a) x100, b) x200, c) and d) x500.

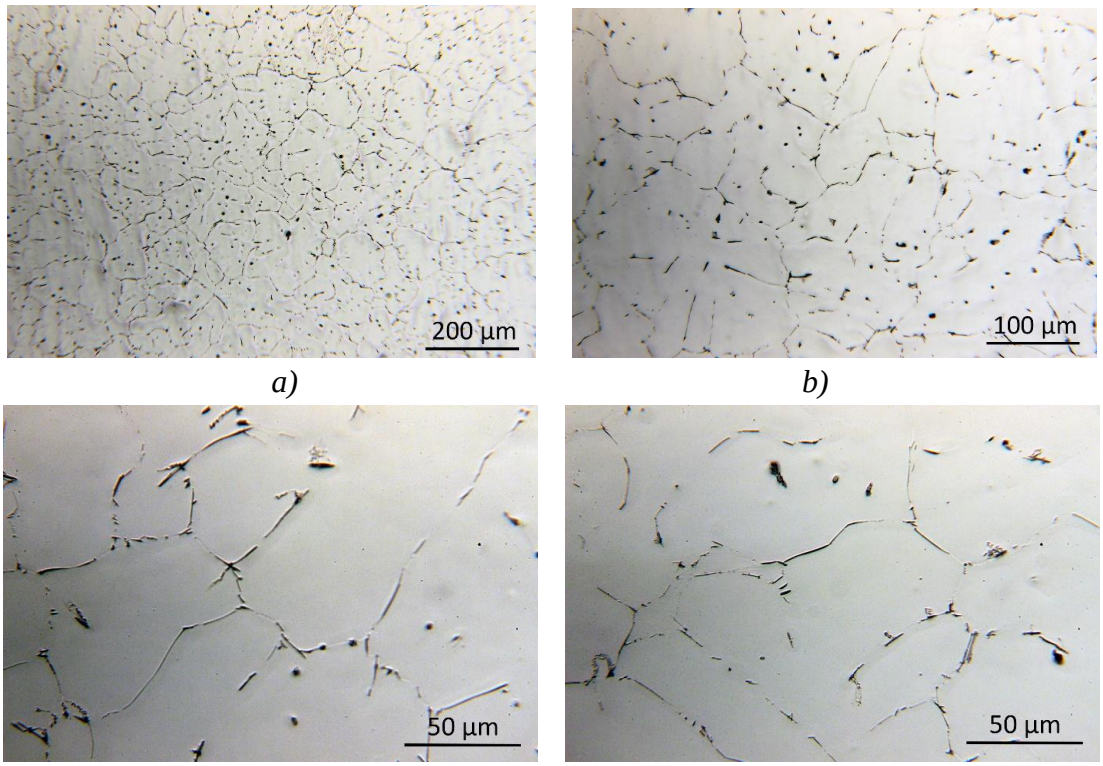

a) *b)*

c) *d)*

Figure 18: Metallography of as-cast Al-alloy 6060, middle section. Magnification: a) x100, b) x200, c) and d) x500.

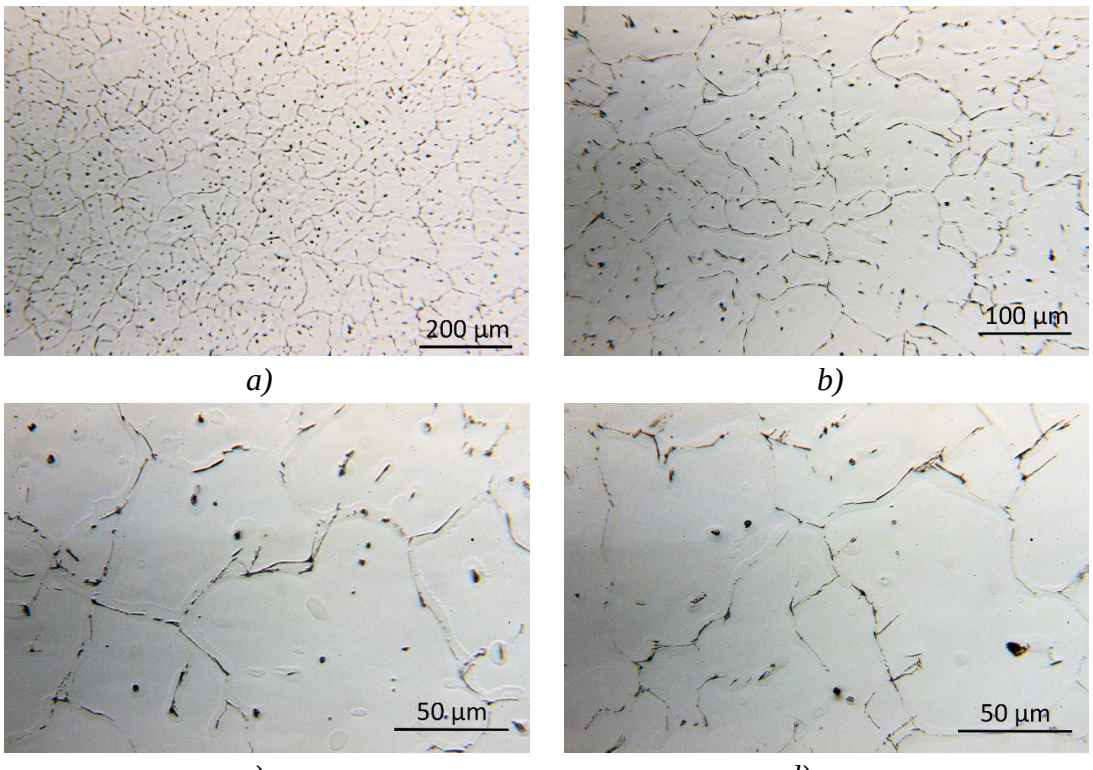

a) *b)*

c) *d)*

Figure 19: Metallography of as-cast Al-alloy 6060, edge section. Magnification: a) x100, b) x200, c) and d) x500.

Scanning electron micrographs of the as-cast material are shown in *Figure 20*, at different magnification levels. By EDX point analysis on the intermetallics, it was observed that the most of them were β-AlFeSi ($Al_9Fe_2Si_2$) and Mg_2Si and a small amount of α-AlFeSi (Al_8Fe_2Si), $Al_{18}Fe_2Mg_7Si_{10}$ (π-phase) and eutectic mixtures. The Mg_2Si particles formed during solidification are large irregularly shaped, as shown in *Figure 20a, b, c and d*, with the dark color. Fine precipitates of Mg_2Si are expected after solidification, but their size is undetectable using SEM and EDX analysis. The most of the particles observed are β-AlFeSi in an elongated morphology near grain boundaries, as shown in *Figure 20c*. Also, smaller rounded particles were formed, which represent β-AlFeSi compounds or more rarely α-AlFeSi, as depicted in *Figures 20e and f*. The π-phase particles are in contact with β-AlFeSi particles and eutectic mixtures, as shown in *Figures 20g and h.* The eutectic particles are formed at the end of solidification, as remaining liquid solidifies isothermally. The phases included in the eutectic mixture, contain β-AlFeSi, Mg_2Si, π-phase and Diamond (Si), but these phases is difficult to observe individually because of their very fine lamellar structure. The differentiation of the phases was made by comparing the ratio of alloying elements of each particle, measured via EDX analysis by SINTEF. The theoretical α-AlFeSi *Fe/Si* is equal to 2.05 and the theoretical β-AlFeSI *Fe/Si* is equal to 0.922.

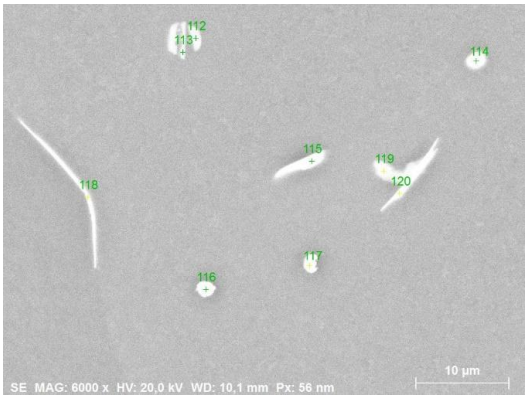

a)

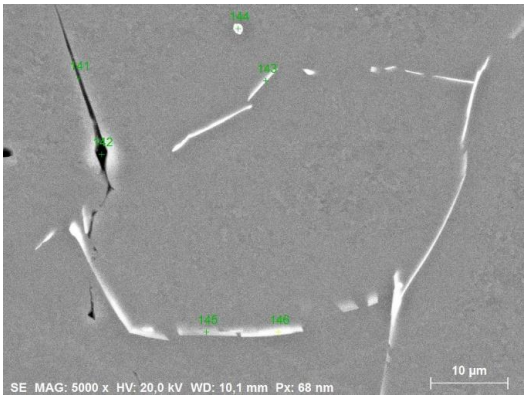

b)

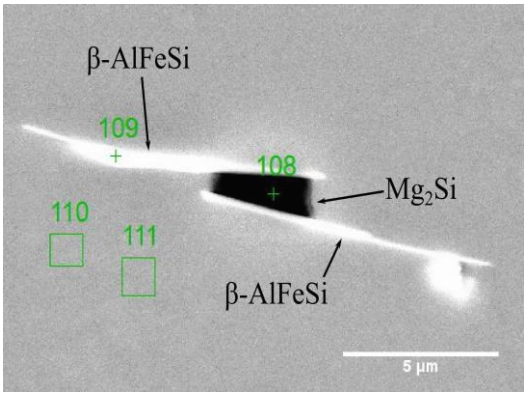

c)

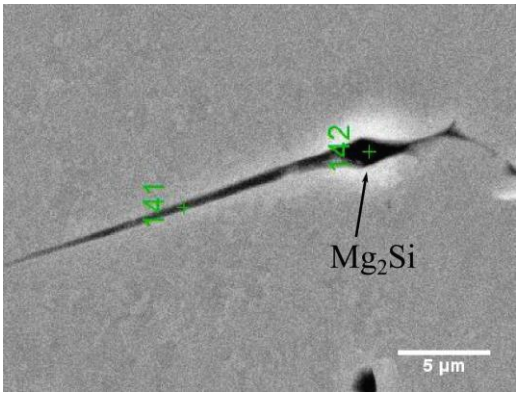

d)

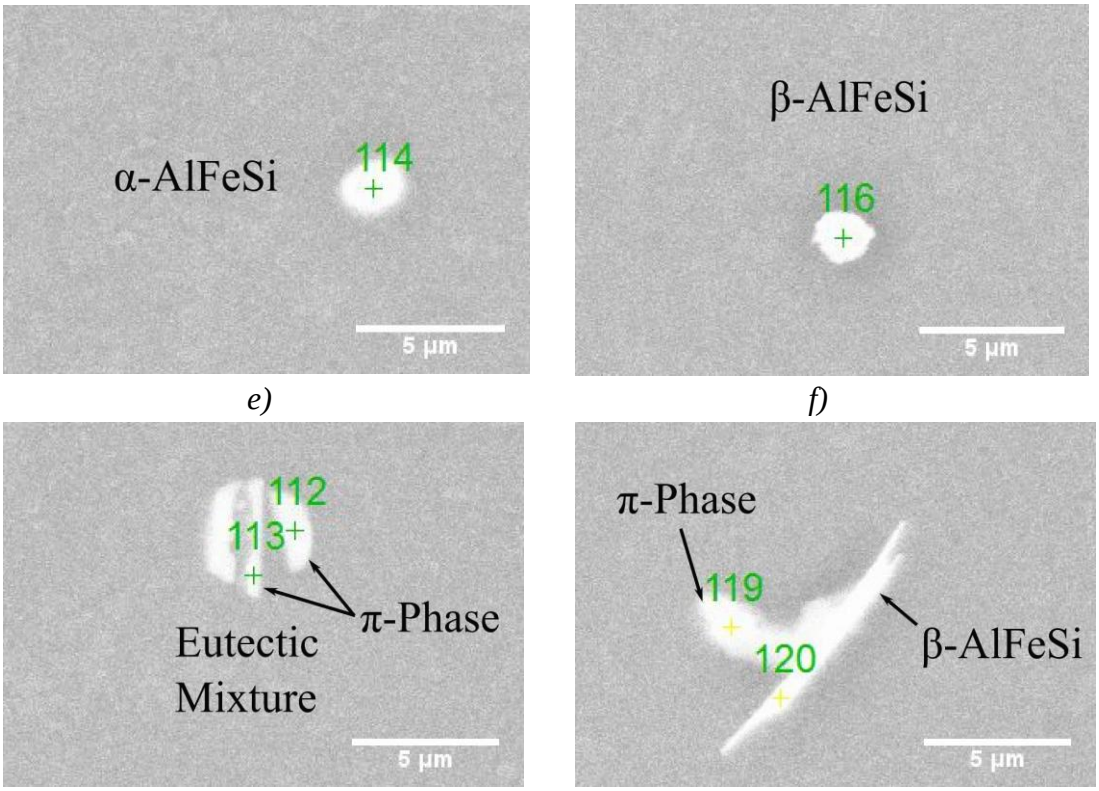

e) *f)*

g) *h)*

Figure 20: Scanning Electron Micrographs of the as-cast material, showing a), b) the intermetallic phases near grain boundary, b), c), d), e), f), g), h) the phases shown in a)and b) separately.

Homogenization is being done in order to increase the extrudability and strength of the alloy by the elimination of the as-cast morphology. While the β-AlFeSi-to-α-AlFeSi transformation plays a critical role to increasing extrudability, the dissolution and re-precipitation of Mg_2Si is one of the main strengthening factors of the Al-alloy. The elimination of sharp and crack inducing β-AlFeSi particles in conjunction with the coarsening of Mg_2Si particles throughout the material body, results to a more extrudable and strong material. The validity of the homogenization simulation was performed via experimental measurements of the as-homogenized material received from industry. The characterization of the as-homogenized material was performed by SINTEF, using Scanning Electron Microscopy (SEM), Energy Dispersive X-Ray point analysis (EDX) and image analysis. Metallographic analysis of the as-homogenized material, using Light Optical Microscopy was performed at the Laboratory of Materials at the University of Thessaly. Samples from the center, middle and edge of the billet along the radius, as shown in *Figure 21*, were analyzed to determine the fraction and morphology of the intermetallic phases that exist and the composition of these phases, after homogenization process.

Figure 21: As-homogenized Al-alloy 6060, sections of received as-homogenized for the characterization analysis.

The microstructure of the as-homogenized material via Light Optical Microscopy at the billet center, middle and edge are shown in *Figures 22, 23 and 24*, respectively. Metallographic images are presented at three different magnification levels, x100, x200 and x500. No significant variations along the billet radius were observed, as shown in *Figures 22, 23 and 24.* The dendritic structures that were present in the as-cast microstructure have been eliminated and the segregation of alloying elements was removed during homogenization. Also, no eutectic particles were observed, because they were completely dissolved during homogenization heating. Regarding the iron intermetallics found near grain boundaries and in between secondary dendritic arms, it was observed that they were more rounded in edges with pinching of elongated particles and partial segmentation into smaller particles. Also, some particles with high aspect ratio observed because of incomplete homogenization.

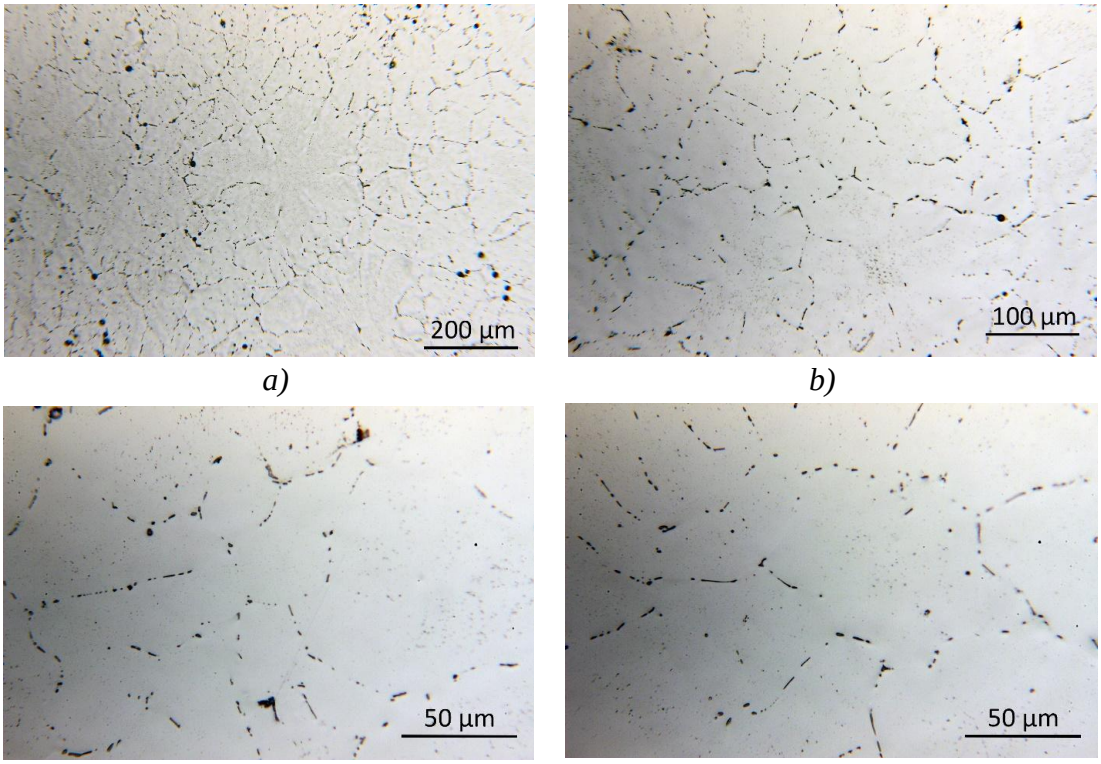

a) *b)*

c) *d)*

Figure 22: Metallography of as-homogenized Al-alloy 6060, center section. Magnification: a) x100, b) x200, c) and d) x500.

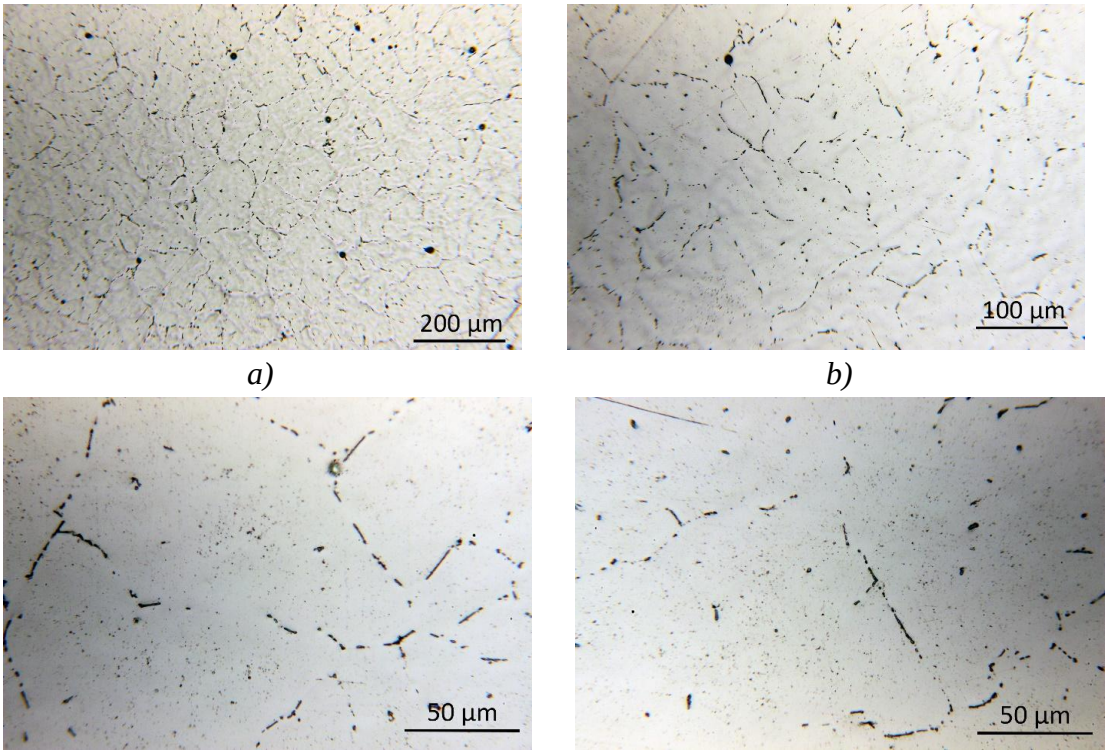

a) *b)*

c) *d)*

Figure 23: Metallography of as-homogenized Al-alloy 6060, middle section. Magnification: a) x100, b) x200, c) and d) x500.

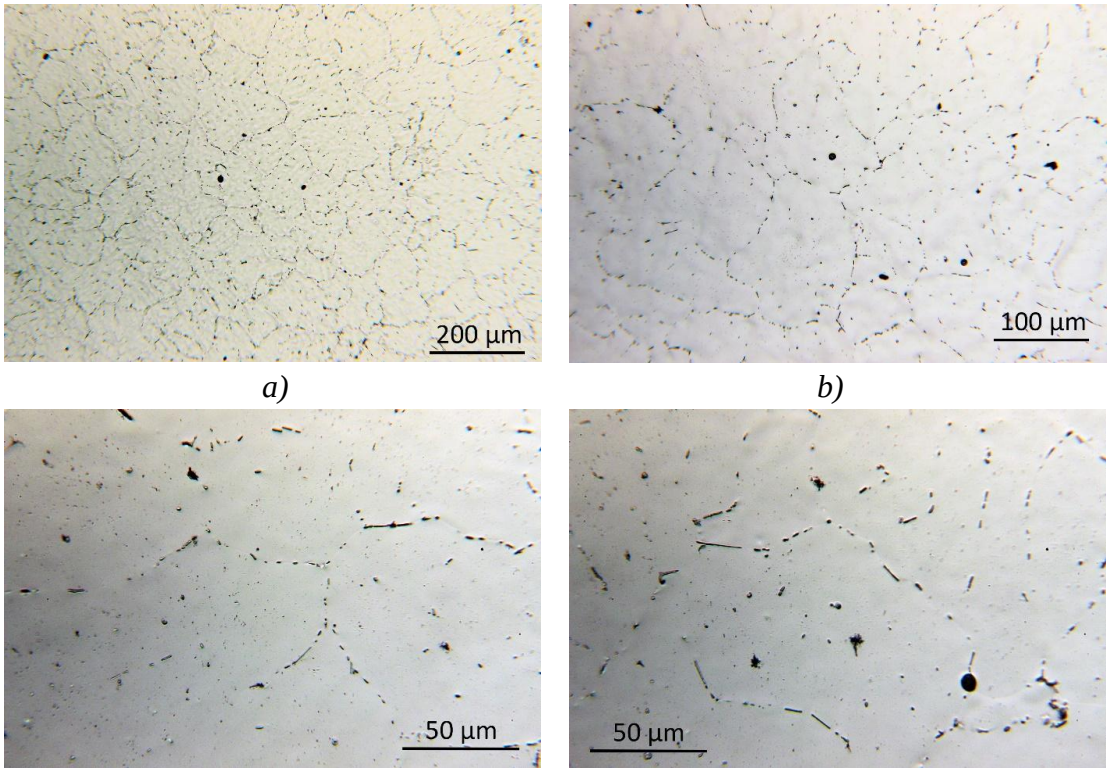

a) *b)*

c) *d)*

Figure 24: Metallography of as-homogenized Al-alloy 6060, edge section. Magnification: a) x100, b) x200, c) and d) x500.

SEM and EDX analysis was conducted by SINTEF in the as-homogenized material in order to measure the volume fraction of phases and determine the homogenization state of the material and the elimination of elemental segregation. Scanning Electron Micrographs of the as-homogenized material are shown in *Figure 25*, at different magnification levels. The volume fraction of intermetallic compounds is reduced compared to the as-cast microstructure. By EDX point analysis on the intermetallics, it was observed that the major intermetallic phases after homogenization treatment were coarse Mg_2Si and α-AlFeSi. Fine precipitates can also exist, but their size is undetectable using SEM and EDX analysis. No significant fractions of β-AlFeSi, π-phase and eutectic mixtures were observed, indicating that the β-to-α transformation is complete. The particles in the as-homogenized microstructure are smaller compared to the as-cast. The spheroidization of α-AlFeSi has not been fully achieved, as shown in *Figures 25b and c*. Most of the α-AlFeSi particles present signs of early stage spheroidization, as the edges of particles were rounded and pinching, forming a neck structure, as shown in *Figure 25b*. Also, dispersoids were found in the grains of the as-homogenized material, white colored small particles, as depicted in *Figure 25d*, but their size and volume fraction was undetectable using EDX point analysis. It is estimated that the dispersoids are α-Mn rich particles of α-AlFeSi, because they have more Mn and they were formed during homogenization holding and cooling. These particles inhibit recrystallization after extrusion and improve the grain structure. The differentiation of the phases was made by comparing the ratio of alloying elements of each particle, measured via EDX analysis by SINTEF. The theoretical α-AlFeSi *Fe/Si* is equal to 2.05 and the theoretical β-AlFeSI *Fe/Si* is equal to 0.922.

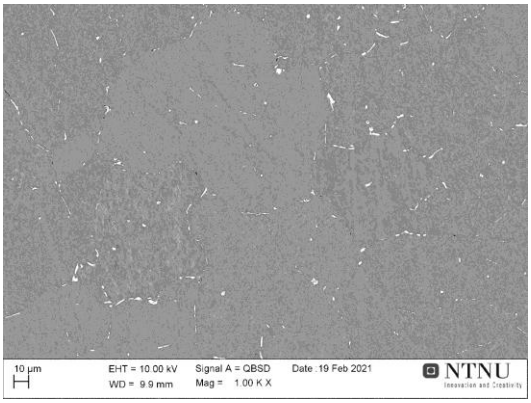

a)

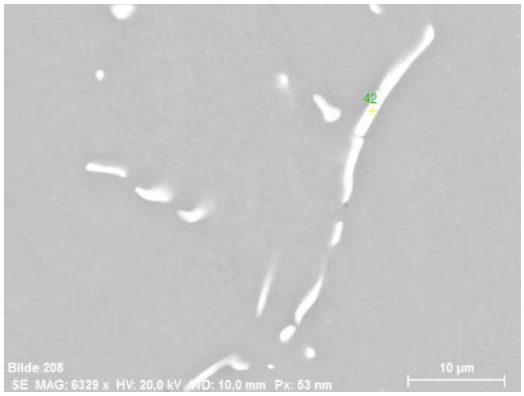

b)

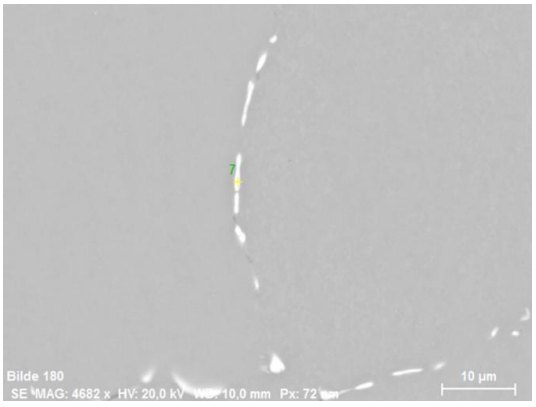

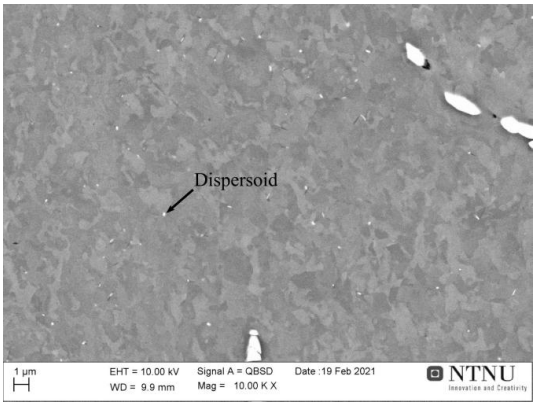

c) *d)*

Figure 25: Scanning Electron Micrographs of the as-homogenized material, showing the microstructure at different magnification levels. Only large Mg_2Si and α-AlFeSi were observed in a), the only iron intermetallic was α-AlFeSi in b), c) and dispersoids were observed in d).

According to EDX measurements of chemical composition of intermetallic phases, it was observed that only α-AlFeSi and large Mg_2Si particles were formed during homogenization. As a result, the transformation of β-to-α AlFeSi is complete and the eutectic mixtures and π-phase particles have been dissolved in α-Al matrix. Fine precipitates of Mg_2Si can also exist after homogenization, but their size is undetectable using SEM and EDX analysis. Dispersoids also observed, most likely comprised of a Mn and Cr rich τ9 structure (also known as α-Mn or $Al_{15}Si_2M_4$), but their size and volume fraction was undetectable using EDX point analysis.

In contrast to experimental observation, the homogenization simulation predicts that the transformation of β-to-α AlFeSi is incomplete. Considering that the maximum homogenization temperature of 570^oC, as measured by industry, remains below the solvus temperature of β-AlFeSi, $T_{sol.\beta\text{-}AlFeSi}=573.3^oC$, is reasonable to observe β-AlFeSi intermetallic phase in the results. If the Nominal Homogenization Temperature of 580^oC is used in the simulations, the completion of β-to-α AlFeSi transformation can be predicted and only α-AlFeSi particles can be observed. This indicates that most likely the temperature measurements were inaccurate and not representative of the temperature experienced by the billets in the homogenization furnace, giving lower measurements. Additionally, the complete dissolution of eutectic mixtures and Mg_2Si particles is predicted by simulation during homogenization heating.

During homogenization cooling the inverse transformation α-to-β AlFeSi is predicted leading to the complete consumption of α-AlFeSi. This behavior is probably not realistic, as the model overestimates the transformation kinetics of the α-to-β AlFeSi under rapid cooling rates. Also, during homogenization cooling the precipitation of Mg_2Si particles is predicted and observed experimentally. The precipitation kinetics of Mg_2Si is overestimated. The homogenization cooling can be simulated using PRISMA, which is not included in this project.

To conclude with, the simulation predictions and experimental observation at the end of homogenization process have some differences. As a result, the homogenization simulation should adjust, using as homogenization holding temperature the nominal Homogenization Temperature of 580^oC. This temperature is the maximum temperature observed during homogenization. Also, the $Al_{18}Fe_2Mg_7Si_{10}$ (π-phase) should be considered to the phases formed during homogenization.

3.5. Updated Homogenization Model

The Solidification Cooling and Homogenization Models were updated according to the experimental findings, to better describe the microstructural evolution upon

processing. In the updated model, α-Al (FCC), Al_8Fe_2Si (α-AlFeSi), $Al_9Fe_2Si_2$ (β-AlFeSi), Mg_2Si, Diamond (Si) and $Al_{18}Fe_2Mg_7Si_{10}$ (π-phase) intermetallic phases were considered during diffusion calculations. The $Al_{18}Fe_2Mg_7Si_{10}$ (π-phase) intermetallic phase was added to diffusion calculations in order to adjust the previous Homogenization Model to the experimental observations. Also, homogenization simulation was performed using the Nominal Homogenization Temperature of 580^oC as the maximum homogenization holding temperature in the cycle, to correct for the low temperature measurements reported. Additionally, to avoid numerical instabilities arising from a eutectoid reaction, involving the Diamond and π-phase at low temperatures, the lowest temperature considered during solidification cooling was kept at 200^oC .

Results regarding the evolution of phase fractions and the composition of the α-Al matrix, during solidification cooling and homogenization heating and holding, is shown in *Figure 26*. The local phase fractions of intermetallic phases as a function of distance in the diffusion cell, at selected times are presented in *Figure 27*. The local chemical composition of the α-Al matrix, indicating the degree of segregation, is given as a function of distance in the diffusion cell, at selected times, in *Figure 28*. The right side of the diffusion cell corresponds to the center of the primary dendrite, whereas the left side represents the end of the dendrite arm, near the grain boundary, where the last liquid was solidifies. Results from Scheil-Gulliver simulations were used to obtain the initial phase fractions and compositions, as shown *in Figures 27a, 28a*. The intermetallic phases formed near the grain boundary where the liquid solidifies at the lowest temperature. A mixture of intermetallic phases is found in the right side of the diffusion cell, according to the solidification sequence:

FCC Al-matrix→ Al_8Fe_2Si(α-AlFeSi) → $Al_9Fe_2Si_2$(β-AlFeSi) → Mg_2Si→ $Al_{18}Fe_2Mg_7Si_{10}$ →Diamond

After solidification, the segregation of alloying elements near the grain boundaries is depicted in *Figure 28a*, where Si and Mg concentrations in the Al-matrix reach a value of 1.35% and 1.05%wt, respectively.

During cooling to room temperature after solidification, according to the temperature curve, given in *Figure 26a,* the volume fraction of Al_8Fe_2Si (α-AlFeSi) decreases significantly, whereas the volume fractions of β-AlFeSi, Mg_2Si, $Al_{18}Fe_2Mg_7Si_{10}$ (π-phase) and Diamond (Si) increase. The α-AlFeSi dissolves completely and re-precipitates and grows at late stages of homogenization. As the function of intermetallic compounds increase during cooling and oversaturation of alloying elements decreases, as shown on *Figures 26c, d,* thus, the segregation profiles of the α-Al matrix decrease. It should be noted that the predicted phase fractions at the end of cooling might be lower and supersaturation of the α-Al matrix higher in practice because the model might overestimate the formation kinetics of intermetallic compound under rapid cooling rate.

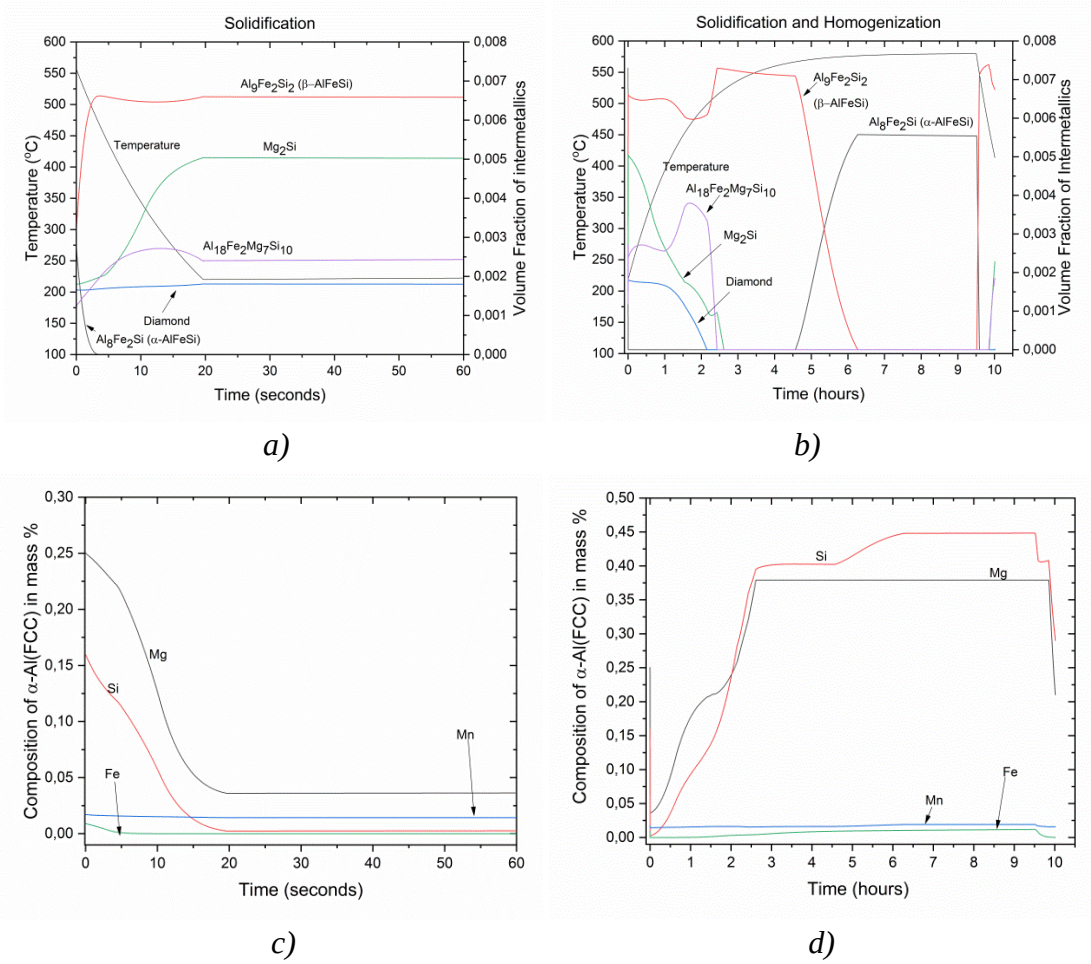

Figure 26: Evolution of a) phase fractions during solidification cooling, b) phase fractions during homogenization, c) composition of the α-Al matrix during solidification, d) composition of the Al-matrix during homogenization.

During homogenization heating, the small fraction of Al_8Fe_2Si (α-AlFeSi) dissolves rapidly, while the fraction of $Al_9Fe_2Si_2$ (β-AlFeSi), Mg_2Si, π-phase and Diamond (Si) slowly decreases, because in low temperatures diffusion is sluggish, as shown in *Figure 26b*. As intermetallic phases dissolve, alloying elements are released in the matrix and the concentration of Al-matrix increases, as shown in *Figure 26d*. By the increase of temperature, the eutectic mixture, containing β-AlFeSi, Mg_2Si, $Al_{18}Fe_2Mg_7Si_{10}$ (π-phase) and Diamond (Si), decreases in fraction and after 2.2 hours of treatment the Diamond (Si) is eliminated, as shown in *Figures 26b and 27c, d*. The $Al_{18}Fe_2Mg_7Si_{10}$ (π-phase) decreases in fraction as the temperature increases and after 2.5 hours of treatment, the π-phase dissolves completely, as shown in *Figures 26b and 27c, d*. The Mg_2Si are initially spheroidized and later dissolved completely at 2.6 hours of heating, as depicted in *Figure 26c, 27c, d*. The dissolution of Mg_2Si, $Al_{18}Fe_2Mg_7Si_{10}$ (π-phase) and Diamond (Si), results in the exaggeration of segregation profiles, because alloying elements are released in the matrix, as depicted in *Figures 28c, d*. As these phases are eliminated, the release of Mg and Si stop, forming a plateau in the composition of the α-Al matrix, as shown in *Figure 26d*. During homogenization, as the temperature increases, the segregation of alloying

elements is eliminated, because they diffuse in the matrix and composition becomes homogeneous, as shown in *Figures 28e-j*.

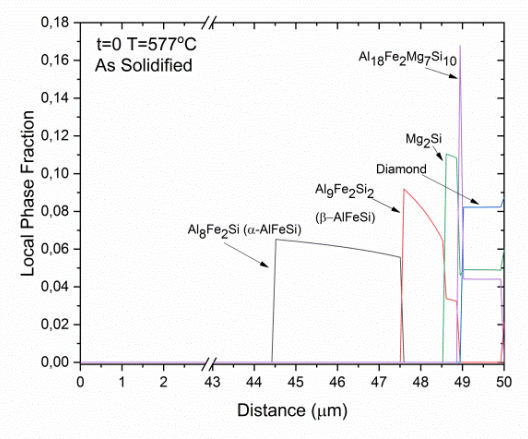

a)

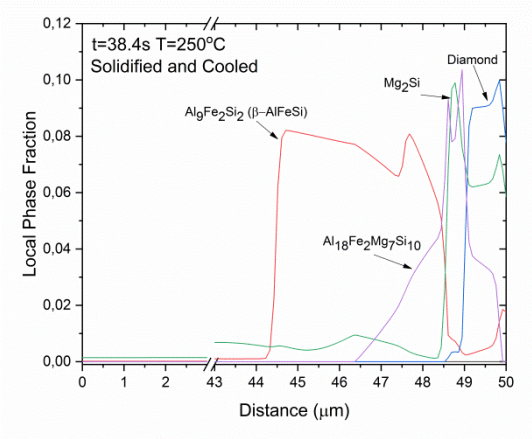

b)

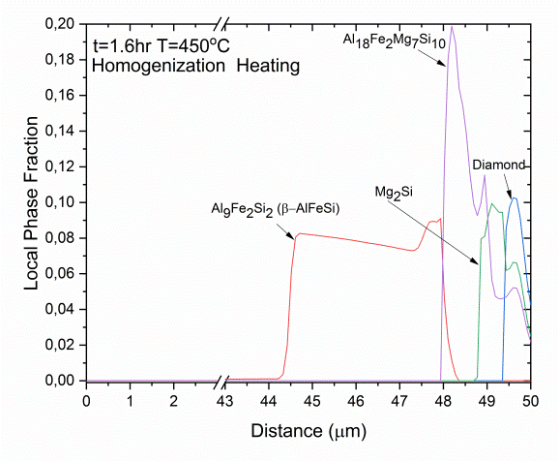

c)

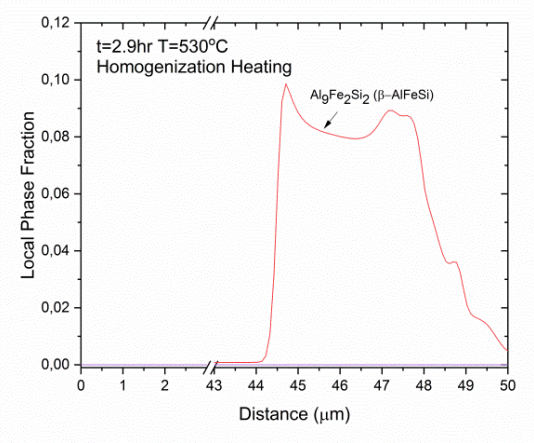

d)

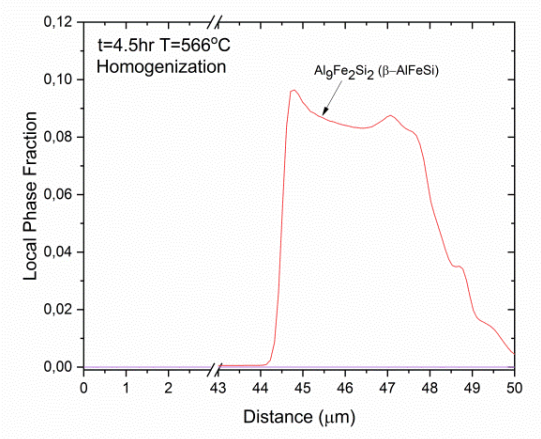

e)

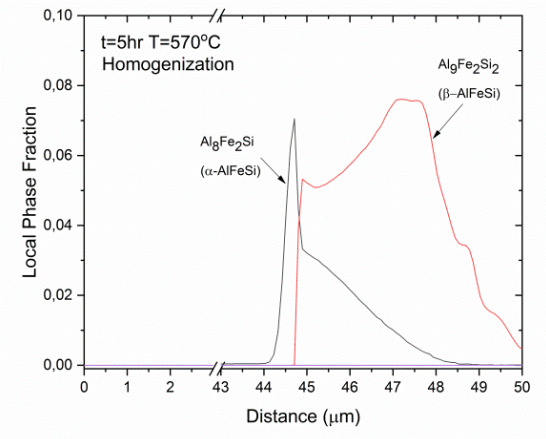

f)

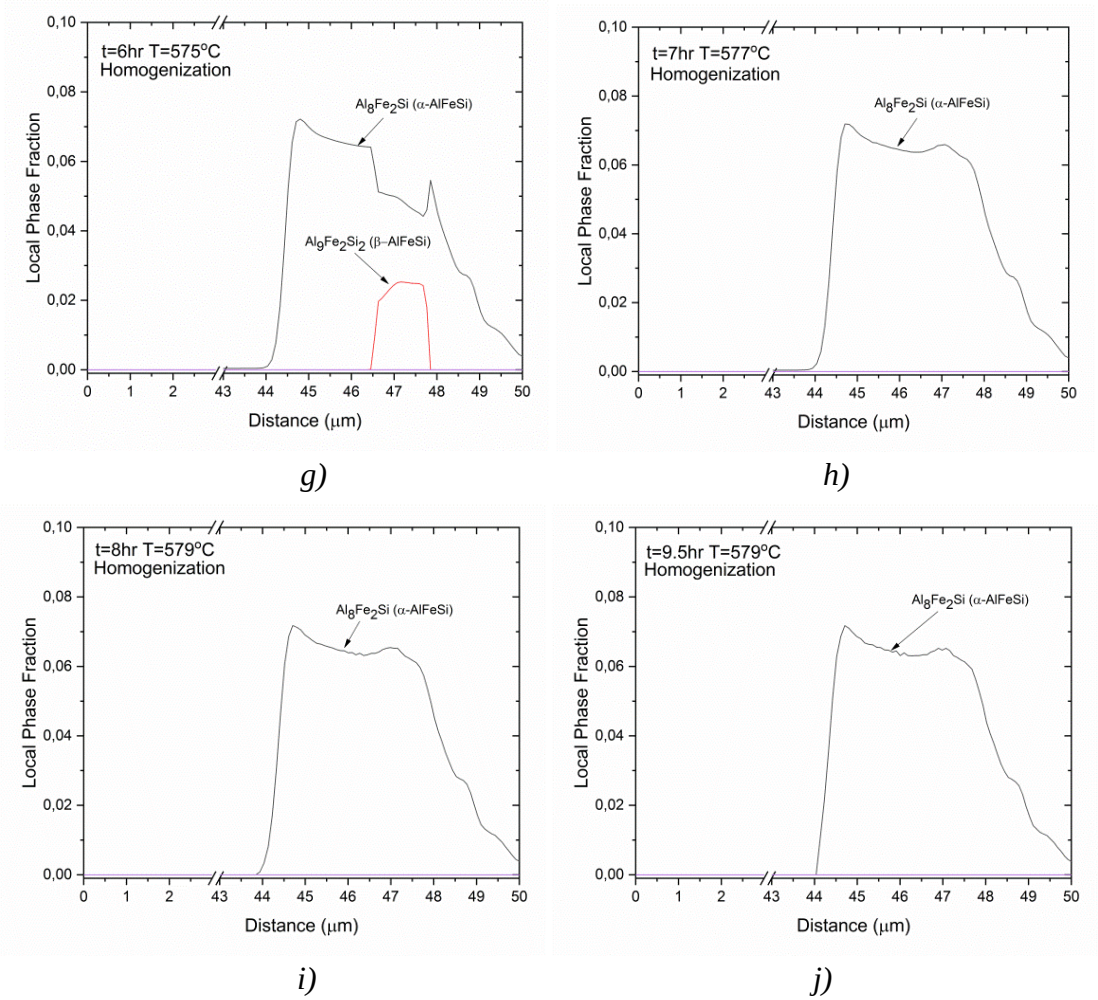

Figure 27: Local intermetallic phase fractions as a function of distance in the diffusion cell, at various times during homogenization treatment. The right side of the cell corresponds to the center of the primary dendrite, whereas the left side to grain boundary.

After the dissolution of the Mg_2Si, $Al_{18}Fe_2Mg_7Si_{10}$ (π-phase) and Diamond (Si), the β-AlFeSi is the main intermetallic compound, with a minimal decrease in phase fraction during homogenization heating and holding, as shown in *Figures 27d, e.* During homogenization holding, the composition of α-Al matrix remains relatively constant, as shown in *Figures 28e-j*. At 5 hours of homogenization process, the α-AlFeSi nucleates together with the β-AlFeSi and begins to grow as the temperature increases, as the β-to-α transformation is favored. During homogenization holding at temperature approximately 580°C, the α-AlFeSi grows against the β-AlFeSi, as depicted in *Figure 27f, g*, while the composition of α-Al matrix remains stable, as shown in *Figure 28f, g*.

At the end of homogenization holding, the only stable phase is the α-AlFeSi, because the β-to-α AlFeSi transformation is complete. The Mg_2Si re-precipitates during homogenization cooling in a fine precipitate with small particle size. During homogenization cooling, the temperature decreases rapidly and this process can be simulated using PRISMA, which is not included in this project.

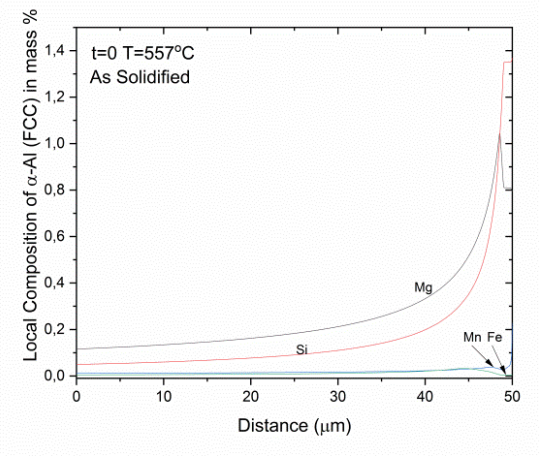
t=0 T=557°C
As Solidified
Local Composition of α-Al (FCC) in mass %
Distance (μm)
Mg
Si
Mn
Fe

a)

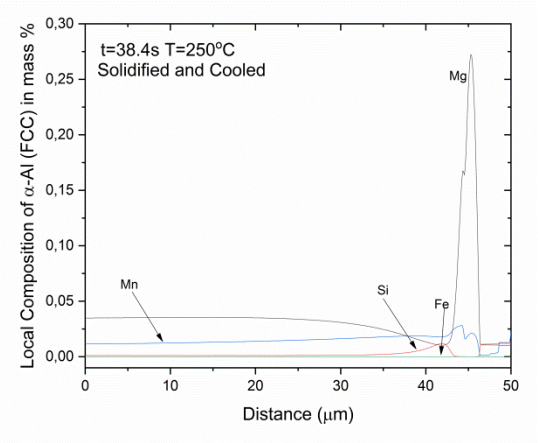
t=38.4s T=250°C
Solidified and Cooled
Local Composition of α-Al (FCC) in mass %
Distance (μm)
Mg
Mn
Si
Fe

b)

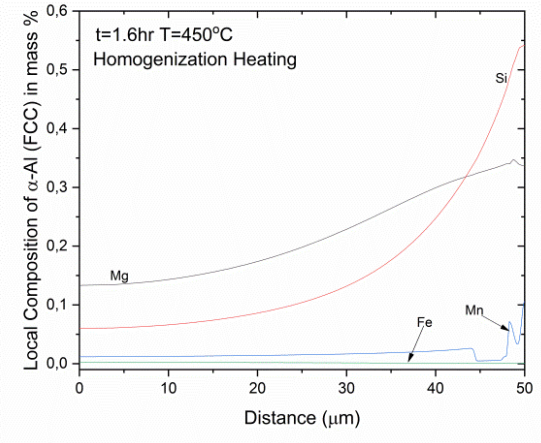
t=1.6hr T=450°C
Homogenization Heating
Local Composition of α-Al (FCC) in mass %
Distance (μm)
Si
Mg
Fe
Mn

c)

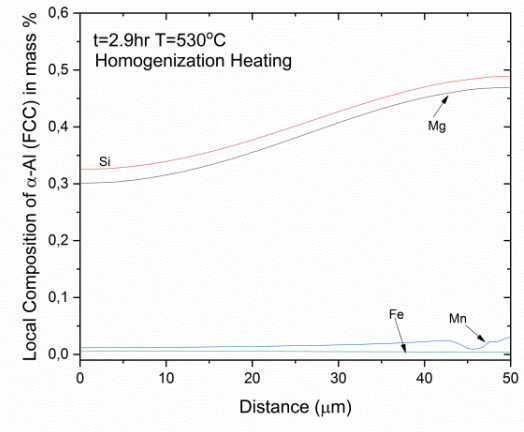
t=2.9hr T=530°C
Homogenization Heating
Local Composition of α-Al (FCC) in mass %
Distance (μm)
Si
Mg
Fe
Mn

d)

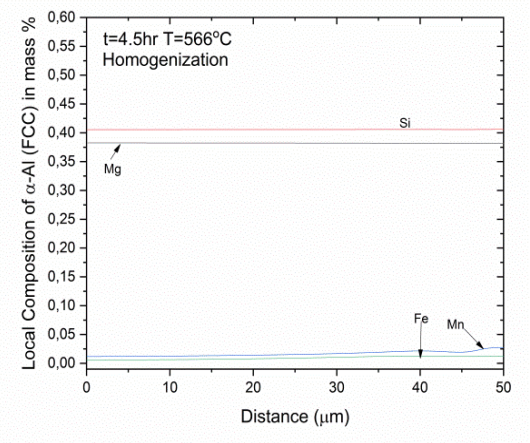
t=4.5hr T=566°C
Homogenization
Local Composition of α-Al (FCC) in mass %
Distance (μm)
Si
Mg
Fe
Mn

e)

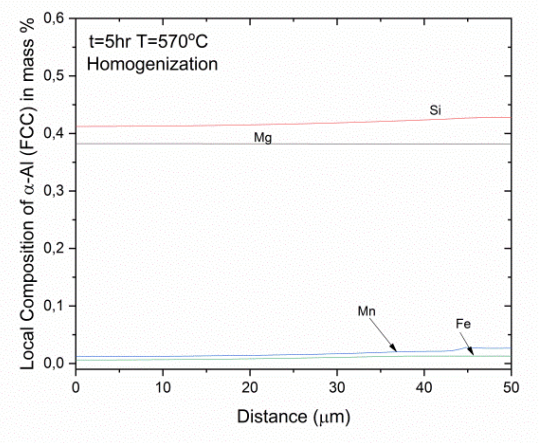
t=5hr T=570°C
Homogenization
Local Composition of α-Al (FCC) in mass %
Distance (μm)
Si
Mg
Mn
Fe

f)

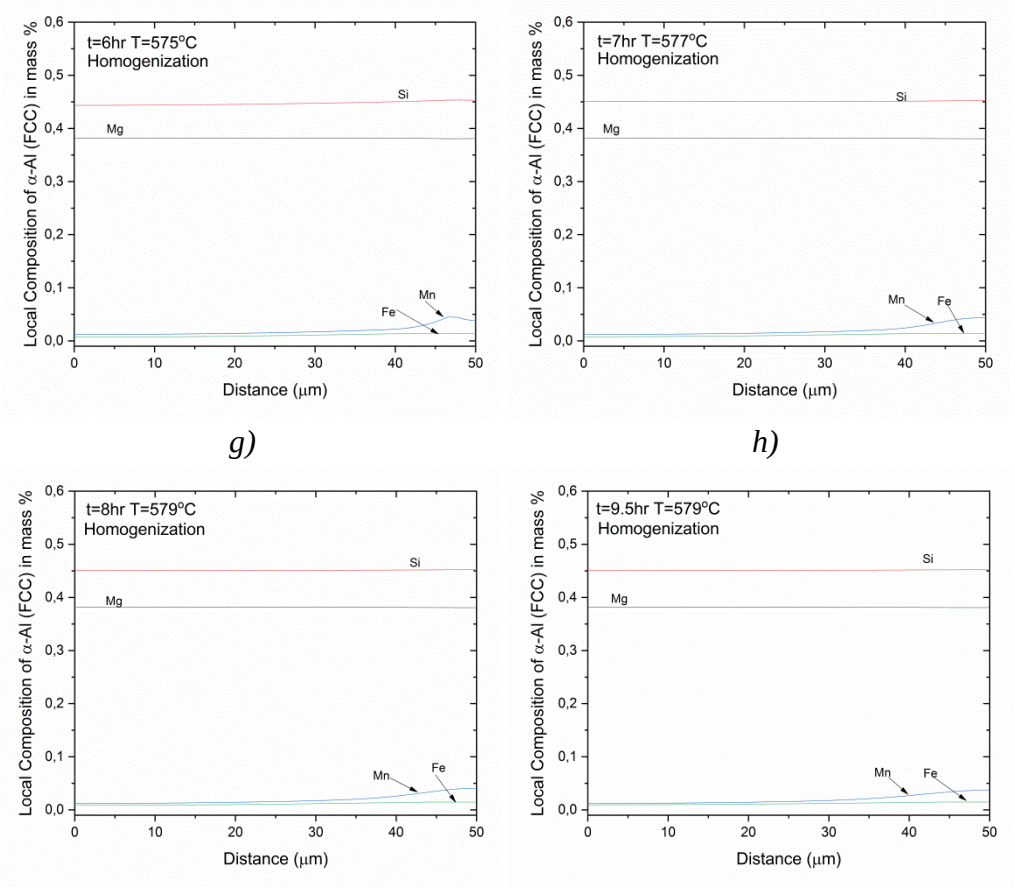

Figure 28: Local composition of the α-Al matrix as a function of distance in the diffusion cell, at various times during homogenization treatment. The right side of the cell corresponds to the center of the primary dendrite, whereas the left side to grain boundary.

3.6. Model Comparison

The volume fraction of phases was measured by SINTEF, via image analysis of micrographs, to validate the predictions of solidification model. The *Table 4* shows the volume fractions of measured and predicted phases after solidification cooling. The fraction of π-phase, α-AlFeSi and eutectic particles was low and difficult to separate from β-AlFeSi. As a result, the volume fraction of π-phase, α-AlFeSi, β-AlFeSi and eutectic particles was measured as ones phase volume fraction, i.e. all white colored particles shown in *Figure 20*. Also, only the particles Mg_2Si forming directly from liquid can be measured, because the Mg_2Si particles which form in eutectic mixtures or during solidification cooling have a very fine structure, undetectable using SEM or EDX analysis. According to model predictions, after solidification cooling, 0.74% of β-AlFeSi, 0.02% of α-AlFeSi, 0.38% of eutectic mixtures and 0.05% of π-phase are present, in total 1.14% for the original simulation model and in total 1.19% for the updated model of these intermetallics, which agrees with the measured value 1.1-1.3%, as shown in *Table 4*. The model prediction for the volume fraction of Mg_2Si in eutectic mixtures is 0.144% and the precipitated fraction is 0.326%. Subtracting the fractions from the total amount of Mg_2Si, 0.56% after

solidification gives 0.09% of Mg_2Si forming directly from liquid, as shown in *Table 4*. The small difference between prediction and measurements, 0.02% can be the result of a limited sample size used for measurements. At the end, the solidification model is in very good agreement with the experimental analysis to the as-cast material.

Table 4: Comparison between measured and predicted phase fractions after solidification cooling

	Measured Vol. Fraction	**Original Model Predicted Vol. Fraction**	**Updated Model Predicted Vol. Fraction**
β-AlFeSi + α-AlFeSi + π-Phase + Eutectics	1.1-1.3%	1.14% (No π-Phase)	1.19%
Blocky β-Mg_2Si	0.014-0.02%	0.09%	0.087%

The volume fraction of phases was measured by SINTEF, via image analysis of micrographs, to validate the predictions of homogenization model. The *Table 5* shows the volume fractions of measured and predicted phases after homogenization process. According to EDX measurements of chemical composition of intermetallic phases, it was observed that only α-AlFeSi and large Mg_2Si particles formed during homogenization. As a result, the transformation of β-to-α AlFeSi is complete and the eutectic mixtures and π-phase particles have been dissolved in α-Al matrix. The fraction of α-AlFeSi was measured at 0.6% and large Mg_2Si particles at 0.026%, slightly higher than the as-cast material, as shown in *Table 5*. Fine precipitates of Mg_2Si can also exist after homogenization, but their size is undetectable using SEM and EDX analysis. According, to model of 580^{o}C Homogenization Holding Temperature predictions, after homogenization process only 0.554% α-AlFeSi are present, because the β-to-α AlFeSi transformation is complete. Additionally, the complete dissolution of eutectic mixtures and Mg_2Si particles is predicted. The difference regarding the Mg_2Si between experimental observation and simulation prediction can be attributed to an inhomogeneous size distribution of Mg_2Si particles, leading to slower dissolution of large particles. At the end, the updated homogenization model is in very good agreement with the experimental analysis to the as-cast material.

Table 5: Comparison between measured and predicted phase fractions after homogenization holding

	Measured Vol. Fraction	**Original Model Predicted Vol. Fraction**	**Updated Model Predicted Vol. Fraction**
α-AlFeSi	0.6%	0.16% (at 570°C)	0.554% (at 580°C)
β-AlFeSi	0%	0.5% (at 570°C)	0% (at 580°C)
β-AlFeSi + α-AlFeSi	0.6%	0.66%	0.554%
Blocky β-Mg_2Si	0.026%	0% (at 570°C)	0% (at 580°C)
Eutectics	0%	0% (at 570°C)	0% (at 580°C)

4. CONCLUSIONS

The solidification and homogenization of the Aluminum alloy 6060 were simulated using kinetic models described above, in order to improve its final properties. Analysis was performed on the Al-alloy 6060, regarding the microstructural evolution during solidification and cooling to room temperature and during homogenization heating, holding and cooling. Microstructural characterization of the as-cast and as-homogenized materials, were conducted using SEM, EDX point and Metallographic analysis.

According to the analysis presented, about solidification the following remarks can be made.

- Solidification begins at the thermodynamic equilibrium liquidus temperature, $T_{liquidus}=654.5^{o}C$, with the nucleation and growth of phases and completes at solidus temperature, $T_{solidus}=557^{o}C$.

- The phase sequence during solidification is:

FCC Al-matrix→ Al_8Fe_2Si (α-AlFeSi) → $Al_9Fe_2Si_2$ (β-AlFeSi) →Mg_2Si→$Al_{18}Fe_2Mg_7Si_{10}$→ Diamond

The phases formed may be individual particles or parts of a eutectic mixture, depending on the solidification temperature. Eutectic mixtures, β-, π-phase particles are large with sharp edges and they limit extrudability.

- During solidification, at 625^{o}C, the α-AlFeSi nucleates and grows until 598^{o}C, where the β-AlFeSi begins to grow. As temperature decreases, the Mg_2Si nucleates at 568^{o}C, the π-phase at 560^{o}C and finally the Diamond (Si) becomes stable at 557^{o}C. Upon solidification, the secondary phases were formed near the grain boundaries.

- Elemental segregation near grain boundaries and at the level of secondary dendritic arms was observed; due to the high cooling rates exist during solidification cooling. The solidified structure represents the as-cast microstructure. Mg concentration drops near grain boundary due to the formation of Mg_2Si and Fe drops due to the formation of α-, β-AlFeSi.

Microstructural evolution during homogenization heating, holding and cooling was performed via multi-component, multi-phase diffusion simulations in DICTRA. According to the analysis presented, about homogenization process the following remarks can be made.

- During homogenization heating, the fraction of Al_8Fe_2Si (α-AlFeSi) dissolves rapidly, while the fraction of $Al_9Fe_2Si_2$ (β-AlFeSi), Mg_2Si and Diamond (Si) slowly decreases, because in low temperatures diffusion is sluggish. Using as Homogenization Holding Temperature of 570^{o}C, the eutectic mixtures dissolve completely after 3 hours of heating. The Mg_2Si particles, formed during solidification dissolve completely after 3.5 hours of treatment. Using as homogenization holding

temperature, the Nominal Homogenization Temperature of 580^oC, the eutectic mixtures dissolve completely after 2.2 hours of heating. The $Al_{18}Fe_2Mg_7Si_{10}$ (π-phase) decreases in fraction and after 2.5 hours of heating, the π-phase dissolves completely. The Mg_2Si particles, formed during solidification dissolve completely after 2.6 hours of treatment. The dissolution of all phases is faster using a higher Homogenization Holding Temperature, as at higher temperatures diffusion is favored.

- The dissolution of Mg_2Si, $Al_{18}Fe_2Mg_7Si_{10}$ (π-phase) and Diamond (Si), results in the exaggeration of segregation profiles, because alloying elements are released in the matrix and the composition of Al-matrix becomes homogeneous.

- Using as Homogenization Holding Temperature of 570°C after 7 hours of process starts the β-to-α AlFeSi transformation. As the temperature increases above 566^oC, the Al_8Fe_2Si (α-AlFeSi) becomes thermodynamically stable and the α-AlFeSi grows against β-AlFeSi without the complete dissolution of the latter, because the temperature remains below the solvus of β-AlFeSi, $T_{solvus\ \beta\text{-}AlFeSi}=573.3^oC$. As a result, the β-to-α AlFeSi transformation is incomplete. Using as homogenization holding temperature, the Nominal Homogenization Temperature of 580^oC, after 5 hours of treatment starts the β-to-α AlFeSi transformation and the α-AlFeSi grows against β-AlFeSi until the complete dissolution of the latter. During homogenization holding, the temperature remains approximately at 580°C which is over the solvus of β-AlFeSi, $T_{solvus\ \beta\text{-}AlFeSi}=573.3^oC$. As a result, the β-to-α AlFeSi transformation is complete.

- The β-to-α transformation kinetics determines the minimum homogenization time because the dissolution of Mg_2Si during homogenization is a fast process while the transformation of β-to-α-AlFeSi is a much slower process. The Mg_2Si particles dissolve completely after 2.6 to 3.5 hours of homogenization treatment whereas the β-to-α transformation starts after 4.5 hours of heating and it is completed after 7 hours of process.

- During homogenization cooling, after 9 hours of treatment, the Mg_2Si particles re-precipitate to an even distribution throughout the body of the alloy with a more homogeneous in-grain distribution. This model overestimates the precipitation kinetics of Mg_2Si under rapid cooling rates. As a result, homogenization cooling can be simulated using a Kampmann-Wagner (KWN) model to better describe the kinetics of nucleation, growth and dissolution of fine particles upon cooling.

- The experimental observation of the as-homogenized samples shows that the phases exist after the end of homogenization treatment, are large Mg_2Si particles and α-AlFeSi. No significant fractions of β-AlFeSi, π-phase and eutectic mixtures were observed, indicating the β-to-α transformation is complete.

- The spheroidization of α-AlFeSi has not fully achieved. Most of the α-AlFeSi particles present signs of early stage spheroidization, as the edges of particles were rounded and pinching, forming a neck structure. Spheroidization of the α-AlFeSi is considered to improve the extrudability of the material. Yet morphological improvements of the remaining α-AlFeSi particles can be achieved via homogenization treatment modifications.

- The material should be heated to a homogenization holding temperature above the solvus temperature of β-AlFeSi, $T_{solvus\ \beta\text{-}AlFeSi}=573.3^oC$, in order to complete the β-to-α transformation. The Nominal Homogenization Temperature of 580^oC is suitable to complete the β-to-α transformation and spheroidize the remaining α-AlFeSi particles. Although, the equilibrium solidus temperature is high at $T_{solidus}=618^oC$, the maximum homogenization temperature should remain below 590^oC to avoid potential partial melting of the material at hot-spots of the surface.

- The homogenization at 580^oC results in the earlier and complete transformation β-to-α compared to the homogenization at 570^oC. At the late stages of homogenization holding at 580°C, 8-9.5 hours of treatment, no significant variations of the volume fraction of the α-AlFeSi observed. So, the homogenization duration can be reduced. Increasing homogenization heating rate to reach solvus temperature of α-AlFeSi and β-AlFeSi earlier, should result in a reduction of the treatment duration, without impact on the final microstructural features.

- The comparison between measured and solidification and homogenization models phase fractions shows agreement, indicating that they can predict the microstructural evolution during solidification and homogenization

5. SUGGESTIONS FOR FUTURE RESEARCH

Some suggestions for further research include the following:

I. Simulation of homogenization cooling using PRISMA.

II. The effect of the ratio of Fe/Si and Mn/Si to the β-AlFeSi to α-AlFeSi phase transformation.

III. Optimization of the homogenization duration when the heating rate increases.

REFERENCES

1. Jin Hu, Majed Jaradeh and Torbjörn Carlberg, Solidification Studies of 6xxx Alloys with Different Mg and Si Contents, Light Metals (2005).

2. Yücel Birol, The effect of Homogenization practice on the Microstructure of AA6063 billets, Journal of Materials Processing (2004), https://doi.org/10.1016/j.jmatprotec.2004.01.056.

*3. Kumar, S., Grant, P.S. & O'Reilly, K.A.Q. Evolution of Fe Bearing Intermetallics During DC Casting and Homogenization of an Al-Mg-Si Al Alloy. Metall Mater Trans A **47,** 3000–3014 (2016). https://doi.org/10.1007/s11661-016-3451-5*

4. Stanislaw Zajac, Bo Bengtsson, Christer Jönsson, Influence of Cooling after Homogenisation and Reheating to Extrusion on Extrudability and Final Properties of AA 6063 and AA6082 Alloys (2002), Materials Science Forum .

5. G.N. Haidemenopoulos, H. Kamoutsi, A.D. Zervaki, Simulation of the transformation of iron intermetallics during homogenization of 6xxx series extrudable Aluminum alloys, Journal of Materials Processing (2012), https://doi.org/10.1016/j.jmatprotec.2012.06.026

6. P.I. Sarafoglou, A. Serafeim, I.A. Fanikos, J.S. Aristeidakis, G.N. Haidemenopoulos, Modeling of microsegregation and homogenization of 6xxx Al-alloys including precipitation and strengthening during homogenization cooling, Materials (Basel). 12 (2019). https://doi.org/10.3390/ma12091421.

*7. Mulazimoglu, M.H., Zaluska, A., Paray, F. et al. The effect of strontium on the Mg_2Si precipitation process in 6201 aluminum alloy. Metall Mater Trans A **28,** 1289–1295 (1997). https://doi.org/10.1007/s11661-997-0265-5.*

8. S. Zajac, B. Hutchinson, A. Johansson & L.-O. Gullman (1994) Microstructure control and extrudability of Al–Mg–Si alloys microalloyed with manganese, Materials Science and Technology, 10:4, 323-333, DOI: 10.1179/mst.1994.10.4.323S.

9. P. Sarafoglou, J. Aristeidakis, M.-I. Tzini, G. Haidemenopoulos, Metallographic Index-Based Quantification of the Homogenization State in Extrudable Aluminum Alloys, Metals (Basel). 6 (2016) 121. https://doi.org/10.3390/met6050121

*10. Andersson, J.O.; Helander, T.; Höglund, L.; Shi, P.; Sundman, B. Thermo_Calc and DICTRA computational tools for materials science. Calphad **2002**, 26, 273–312*

11. Lukas, H.; Fries, S.G.; Sundman, B. Computational thermodynamics, the Calphad method; Cambridge University Press: Cambridge, UK, 2007; ISBN 9780521868112

*12. Shi, R.; Luo, A.A. Applications of CALPHAD modeling and databases in advanced lightweight metallic materials. Calphad **2018**, 62, 1–17*

*13. Bo Sundman, Ibrahim Ansara, III.2 - The Gulliver–Scheil method for the calculation of solidification paths, The SGTE Casebook (Second Edition), Woodhead Publishing, **2008**, 343346, ISBN 9781845692155*

*14. Henrik Larsson, Lars Höglund, Multiphase diffusion simulations in 1D using the DICTRA homogenization model, Calphad, **2009**, 33, 495-501*

*15. Wagner, R.; Kampmann, R. Homogeneous second phase precipitation. In Materials Science and Technology, Vol.5, Phase Transformations in Materials; Cahn, R.W., Haasen, P., Kramer, E.J., Eds.; VCH: Weinhein, Germany, **1991**; p. 21. ISBN 3527268189*

16. Iss, N. and K. V. Sharma, Effect of magnesium on strength and microstructure of Aluminium Copper Magnesium Alloy, Materials Science (2012).

17. Mehdi, Husain. Effect of Silicon content on the Mechanical Properties of Aluminum Alloy. International Research Journal of Engineering and Technology. 2. 1326-1330, (2015).

*18. Nam, S.W., Lee, D.H. The effect of Mn on the mechanical behavior of Al alloys. Metals and Materials **6,** 13 (2000). https://doi.org/10.1007/BF03026339.*

19. Taylor, John. The effect of iron in Al-Si casting alloys. 35th Australian Foundry Institute National Conference, (2004).

20. Thiago M. Ribeiro, Eduardo Catellan, Amauri Garcia, Carlos A. dos Santos, The effects of Cr addition on microstructure, hardness and tensile properties of as-cast Al–3.8wt.%Cu–(Cr) alloys, Journal of Materials Research and Technology,(2020). https://doi.org/10.1016/j.jmrt.2020.04.054.

21. Mukhopadhyay, A.K., Yang, Q.B., & Singh, S.R.. The influence of zirconium on the early stages of aging of a ternary Al-Zn-Mg alloy. Acta Metallurgica et Materialia, 42(9), 3083-3091, (1994).

22. Chakrabarti, D.J., Yingguo Peng, and David E. Laughlin. "Precipitation in Al-Mg-Si Alloys with Cu Additions and the Role of the Q' and Related Phases."

Materials Science Forum 396–402 (2002): 857–62. https://doi.org/10.4028/www.scientific.net/msf.396-402.857.

23. Claves, S.R., D.L. Elias, and Wojciech Z. Misiolek. "Analysis of the Intermetallic Phase Transformation Occurring during Homogenization of 6xxx Aluminum Alloys." Materials Science Forum 396–402 (2002): 667–74. https://doi.org/10.4028/www.scientific.net/msf.396-402.667.

24. Sun Y., Johnson D.R., Trumble K.P., Priya P., Krane M.J.M. (2014) Effect of Mg_2Si Phase on Extrusion of AA6005 Aluminum Alloy. In: Grandfield J. (eds) Light Metals 2014. Springer, Cham. https://doi.org/10.1007/978-3-319-48144-9_73

25. Österreicher, Johannes & Kumar, M. & Schiffl, Andreas & Schwarz, Sabine & Bourret, Gilles. Secondary precipitation during homogenization of Al-Mg-Si alloys: Influence on high temperature flow stress. Materials Science and Engineering (2017).: A. 687. 10.1016/j.msea.2017.01.074.

26. Pikee Priya, Microstructural evolution during the Homogenization heat treatment of 6xxx and 7xxx.